



Published in final edited form as:

J Immunol. 2019 October 15; 203(8): 2150–2162. doi:10.4049/jimmunol.1900832.

Distinct PLZF+CD8 $\alpha\alpha$ ⁺ unconventional T cells enriched in liver use cytotoxic mechanism to limit autoimmunity¹

Huiming Sheng^{*,‡,2}, Idania Marrero^{*,2}, Igor Maricic^{*}, Shaohsuan S. Fanchiang^{*}, Sai Zhang[†], Derek B. Sant'Angelo[†], Vipin Kumar^{*}

^{*}Division of Gastroenterology, Department of Medicine, University of California San Diego, La Jolla, CA 92093, USA

[†]Rutgers University, New Brunswick, NJ 08901, USA

[‡]Current address: Shanghai Jiao Tong University, Shanghai, China

Abstract

Hepatic immune system is uniquely challenged to mount a controlled effector response to pathogens while maintaining tolerance to diet and microbial antigens. We have identified a novel population of innate-like, unconventional CD8 $\alpha\alpha$ ⁺TCR $\alpha\beta$ ⁺ T cells in naïve mice and in human peripheral blood, called CD8 $\alpha\alpha$ T_{unc}, capable of controlling effector T cell responses. They are NK1.1⁺ (CD161⁺ in human), express NK inhibitory receptors and express the promyelocytic leukemia zinc finger (PLZF) transcription factor that distinguishes them from conventional CD8⁺ T cells. These cells display a cytotoxic phenotype and use a perforin dependent mechanism to control antigen-induced or T cell-mediated autoimmune diseases. CD8 $\alpha\alpha$ T_{unc} are dependent upon IL-15/IL-2R β signaling and PLZF for their development and/or survival. They are FoxP3-negative and their regulatory activity is associated with a functionally distinct Qa-1^b-dependent population co-expressing CD11c and CD244. A polyclonal TCR repertoire, an activated/memory phenotype and the presence of CD8 $\alpha\alpha$ T_{unc} in NKT- and in MAIT-deficient, as well as in germ-free mice indicates that these cells recognize diverse self-protein antigens. Our studies reveal a distinct population of unconventional CD8⁺ T cells within the natural immune repertoire capable of controlling autoimmunity and also providing a new target for therapeutic intervention.

Introduction

Liver is a unique organ in that it has a central role in the metabolism and in the maintenance of immune tolerance against a constant exposure to diet and microbial antigens (1). However, at the same time, hepatic immune system needs to provide immunity against chronic infections and cancer metastasis. Thus, immune response in the liver has to be appropriately controlled to avoid excessive tissue damage without compromising the tissue integrity and metabolic functions (2). Liver contains specialized resident immune cells, including tolerogenic antigen-presenting cells (3) as well as adaptive and innate lymphoid

Address correspondence and reprint request to Prof. Vipin Kumar, Department of Medicine, Division of Gastroenterology, University of California San Diego, 9500 Gilman Drive, Medical Teaching Facility Bldg. Room #414, La Jolla, CA 92093. phone number: 858-822-0730, fax number: 858-822-6959, vckumar@ucsd.edu.

²H. Sheng and I. Marrero contributed equally to this work.

cell populations. Particularly, liver is enriched in several innate lymphoid cells that respond rapidly to conserved ligands, including NK cells and unconventional T cells, like NKT cells, mucosal-associated invariant T (MAIT) cells and $\gamma\delta$ T cells (4). Unconventional T cells, distinct from conventional class I or class II MHC-restricted T cells, are generally restricted by non-classical MHC class Ib (e.g., Qa-1^b/HLA-E, H2-M3) and MHC class-I like (e.g., CD1, MR1) molecules and recognize a different class of non-protein antigens, such as self and microbial lipids and metabolites (4). While significantly more is known about the role of NKT or MAIT cells in mounting effector immune responses, little is known about the identity or function of other hepatic innate-like T cells involved in controlling immunity. Knowledge of rapidly-acting innate regulatory mechanism(s) is important in understanding how excessive inflammatory responses are controlled to maintain tissue integrity.

T cells are controlled by both intrinsic (e.g., PD1, anergy and exhaustion) and extrinsic cell-based (Treg) mechanisms that prevent their over-stimulation. While an important role of FoxP3⁺CD4⁺ Treg in homeostasis is abundantly clear (5), the biology of CD8⁺ T cells with regulatory activity is still incompletely understood despite demonstration of their involvement in immune regulation (6-11). A regulatory role for CD8⁺ T cells has also been suggested in various conditions in humans, e.g. in transplant survival (12), inflammatory bowel disease (13) and multiple sclerosis (14, 15). Regulatory CD8⁺ T cells have been identified using cell surface expression of several markers, including CD8 $\alpha\alpha$, CD122, Ly49 and CD11c (9, 16-19). Since, these molecules are also expressed by activated conventional CD8⁺ T cells, one of the major issues curtailing a detailed characterization of regulatory CD8⁺ T cells has been to distinguish them from non-regulatory CD8⁺ T cells.

In this study, for the first time, we have identified a novel, innate-like CD8 $\alpha\alpha$ ⁺TCR $\alpha\beta$ ⁺ polyclonal T cell population enriched in the liver of naïve mice and also present in healthy humans, referred to as CD8 $\alpha\alpha$ T_{unc}, which is distinguishable from conventional CD8⁺ T cells by the expression of the promyelocytic leukemia zinc finger (PLZF) transcription factor. CD8 $\alpha\alpha$ T_{unc} control T cell-mediated autoimmunity using a perforin-dependent mechanism and are comprised of a functionally distinct population that co-express CD11c and CD244. It is noteworthy that CD8 $\alpha\alpha$ T_{unc} are dependent upon IL-2R β signaling and a substantial number of them are Qa-1^b-restricted. In summary, our findings reveal a new member of the unconventional T cells with immune regulatory function that can be potentially targeted for intervention in inflammatory diseases.

Materials and Methods

Ethics statement

Animal studies were carried out in strict accordance with the recommendations of the Guide for the Care and Use of Laboratory Animals of the National Institutes of Health. The protocols were reviewed and approved by the Institutional Animal Care and Use Committee of the University of California San Diego.

Mice

C57BL/6 (B6) as well as IL-6^{-/-}, IL-15^{-/-}, perforin^{-/-}, IFN γ ^{-/-}, Rag1^{-/-} μ MT^{-/-}, T-bet^{-/-}, TAP1^{-/-}, athymic nude mice and OT-II Tg mice on a B6 background were purchased from The Jackson laboratory (Bar Harbor, MI). Qa-1^b^{-/-} mice (originally provided by Dr. Peter Jensen, University of Utah) and CD1d^{-/-}, J α 18^{-/-} and MR1^{-/-} mice (originally provided by Dr. Mitch Kronenberg, La Jolla Institute for Immunology, La Jolla, CA), all on a B6 background, were bred in our own facility. PLZF^{-/-}, PLZF-eGFP (PEG) reporter mice and PCre x R26T mice were provided by Dr. Derek Sant'Angelo, Rutgers University, New Jersey. CD8 α ^{-/-} and CD8 β ^{-/-} mice were kindly provided by Dr. Dan Littman (NYU). CD25^{-/-}, CD122^{-/-} and IL-7^{-/-} mice were provided by late Dr. Charlie Surh (TSRI). Mice were housed in individually ventilated cages and used at 6–12 wks of age.

Healthy donors

Cryopreserved PBMC cells from 25 healthy donors were purchased from either Gelantis or iXCells Biotechnologies (San Diego, CA). PBMC were purified from whole blood by density gradient centrifugation.

Cell isolation

MNCs from livers were isolated using mechanical crushing through a 70 μ m cell strainer followed by Percoll gradient separation and RBC lysis as described (20). MNCs from lung were isolated by cutting the organs into small pieces following by homogenization using gentleMACS tubes and gentleMACS Dissociator (Miltenyi). The homogenate was mashed through a 100 μ m cell strainer in a 50 ml conical tube, washed and resuspended in 35% Percoll solution (GE Healthcare Life Sciences) containing 100 U/ml of heparin. Gradient was centrifuged at 2000 rpm for 15 min at room temperature. The supernatant was removed and erythrocytes were lysed. MNCs from spleen and thymus were isolated by grinding the organs through 70 μ m cell strainer and lysed of RBC prior to staining. Isolated MNCs from different organs were counted with a hemocytometer using trypan blue staining. PBMC was collected from the tail veins of mice prior to euthanasia. Blood samples were immediately lysed using Red Blood Cell Lysis Buffer (Millipore Sigma), washed, and suspended in PBS prior to staining.

Flow cytometry

For mice experiments, single cell suspensions were first incubated with anti-CD16/CD32 (Fc BlockTM) in FACS buffer (0.02% sodium azide/2% FBS/PBS) and stained with antibodies against CD45R/B220 (clone RA3–6B2), CD4 (GK1.5 or RM4–5), TCR β (H57–597), CD8 α (53–6-7), CD8 β (YTS156.7.7), CD8 β .2 (53–508), CD45RB (C363.16A), CD69 (H1.2F3), NK1.1 (PK136), CD44 (IM7), CD62L (MEL-14), PLZF (21F7), Foxp3 (3G3), GITR (DTA-1), CD25 (7D4), CD122 (TM- β 1), CD127 (A7R34), PD1 (J43), CD28 (37.51), CD27 (LG.3A10), CD200 (OX-90), OX40 (OX-86), ICOS (HK5–3), CXCR5 (2G8), Eomes (Dan 11 mag), CD103 (2E7), LY49A (A1), Ly-49E/F (CM4), Ly-49G (AT-8), Ly-49G2 (LGL-1), Ly-49I (YLI-90), Ly-49D (4E5), Ly49H (3D10), CD244 (eBio244F4), CD11c (HL3), and CD314 (NKG2D or CX5) which were purchased from BD Biosciences (BD), Biolegend or Thermo Scientific. TCR V α or V β usage was determined by flow

cytometry using either antibodies against V α 2 (B20.1), V α 3.2 (RR3–16), V α 8.3 (B21.14) and V α 11.1 (RR8–1) or Mouse V β TCR screening panel (BD). Intracellular cytokine staining was performed using the BD Cytotfix/Cytoperm plus Fixation/Permeabilization Kit with BD GolgiStop according to manufactures protocol. Briefly, after stained for cell surface markers, cells were permeabilized for 20 min with the Fixation/permeabilization buffer on ice, washed twice in perm/wash buffer, and stained with intracellular antibodies for 30 min on ice. For human experiments, PBMC were first incubated in FACS buffer (0.1% sodium azide/1% human AB serum/1% FBS/PBS) and stained with antibodies against TCR $\alpha\beta$ (T10B9.1A-31), CD8 α (RPA-T8), CD8 β (2ST8.5H7), PLZF (R17–809), CD161 (HP-3G10), TCR V α 7.2 (3C10), CD45RA (HI100), CD197(CCR7) (G043H7), CD244 (2–69), CD11c (Bu15), Granzyme B (GB11), Perforin (δ G9), IL-18 R α /IL-1 R5 (70625), ROR γ t (Q21–559), CD186(CXCR6) (K041E5), CD196(CCR6) (11A9), IFN γ (4S.B3), IL-17A (eBio64DEC17), TNF α (MAb11) and IL-4 (MP4–25D2) which were purchased from BD, Biolegend or R&D. For intracellular cytokines and transcription factors staining, PBMC were not *in vitro* stimulated, instead PBMC were first stained directly for cell surface markers, then, fixed and permeabilized using BD Pharmingen™ Transcription Factor Buffer Set. Briefly, cells were permeabilized for 45 min with the Fixation/permeabilization buffer on ice, washed twice in perm/wash buffer, and stained with intracellular antibodies for 45 min on ice. Samples were further resuspended in 1x BD Stabilizing Fixative and store at 4°C until acquisition. Cells were analyzed on a FACS Calibur or Canto (BD) at the Flow Cytometry Research Core Facility (Veterans Affairs San Diego Healthcare System, San Diego, CA) and all analysis performed using FlowJo v10 software (TreeStar). PE-conjugated α GalCer/mCD1d tetramers were generated in our laboratory, as previously described (21). Synthetic α GalCer was provided by Kirin Brewery.

Adoptive T cell transfer

For adoptive transfer, CD8 $\alpha\alpha$ T_{unc} and CD8 T_{con} were sorted from liver of B6, CD1d^{-/-} or Perforin^{-/-} mice on a BD FACS Aria II at the Flow Cytometry Research Core Facility following the strategy described in Fig. 1A. For inhibition of EAE, 2×10^5 sorted CD8 $\alpha\alpha$ T_{unc} or CD8 T_{con} from B6 mice or 1×10^5 cells from CD1^{-/-} mice were intravenously (i.v.) injected into recipient mice. To transfer CD8 $\alpha\alpha$ ⁺CD11c⁻ cells, CD11c⁺ cells were first depleted from total CD8⁺ T cells by negative selection using the CD8 α ⁺ T cell isolation kit (Miltenyi Biotech) and then sorted using antibodies against TCR β , CD8 α and CD8 β mAbs. Sorted CD8 $\alpha\alpha$ ⁺CD11c⁻ were i.v. injected into naïve B6 recipient mice (2×10^5 /mouse) one day before EAE induction. For inhibition of colitis, 2×10^5 CD8 $\alpha\alpha$ T_{unc} from B6 or Perforin^{-/-} mice were i.v. injected into Rag1^{-/-} recipient mice.

Induction of EAE

EAE was induced in 8–12-wk-old sex matched B6 mice by immunization with 200 μ g of MOG_{35–55} peptide (MEVGWYRSPFSRVVHLYRNGK) emulsified in CFA (Difco). A total volume of 0.2 ml was injected subcutaneously into the flank, at both right and left sides. On the same day and 48 h later, mice were injected intraperitoneally with 150 ng in 0.2 ml of pertussis toxin (List Biological laboratories). Clinical signs of EAE were assessed daily, as previously described (22) using a five-point scale: 1, flaccid tail; 2, hind-limb weakness; 3, hind-limb paralysis; 4, whole-body paralysis; 5, moribund or death.. The mean disease score

for each group was calculating by averaging the maximum severity of all of the affected animals in the group. In some experiments, HEL₇₄₋₉₀ peptide (NLCNIPCSALLSSDITA) was used instead of MOG₃₅₋₅₅ peptide following the same protocol.

CD45RB^{high} transfer model of colitis

Colitis was induced in 6–8-wk-old sex-matched groups of Rag1^{-/-} mice following i.v. injection of sorted CD4⁺CD25⁻CD45RB^{hi} T cells (4×10^5 cells/mouse) from splenocytes of B6 mice or co-transferred with sorted CD8 $\alpha\alpha$ T_{unc} (2×10^5 /mouse) from either naïve B6 or perforin^{-/-} mice. Recipient mice were weekly weighed and monitored for signs of illness and sacrificed after 8 wk. Colon samples were collected, fixed in formalin, embedded in paraffin and stained with H&E. All samples were scored by researchers “blinded” to the experimental conditions.

CFSE proliferation in vivo assay

OVA-specific CD4⁺ T cells were isolated from spleen of OT-II Tg mice by positive selection using mouse CD4 (L3T4) Microbeads (Miltenyi Biotech). CD8⁺ T cells were positively selected from spleen of B6 mice ($n = 10$) using mouse CD8a (Ly-2) Microbeads (Miltenyi Biotech). Liver MNCs from B6 and perforin^{-/-} mice were isolated as described before. *OT-II cell transfer assay*: positive selected CD4⁺ (OT-II) T cells were CFSE labeled (5 μ M) using Vybrant CFDA SE Cell Tracer Kit (Life Technologies). CFSE-labeled CD4⁺ T cells (1×10^6 cells/200 μ l) were i.v. injected into B6 recipient mice alone or co-injected with positive selected CD8⁺ T cells (10×10^6 cells/mouse) from B6 mice or liver MNCs (8×10^6 cells/mouse) isolated from B6 or perforin^{-/-} mice. After 24 h, recipient B6 mice were intraperitoneally immunized with 50 μ g of OVA₃₂₃₋₃₃₉ peptide (ISQAVHAAHAEINEAGR) in PBS or injected with PBS alone. Three days after stimulation, recipient mice were sacrificed and spleens were analyzed by flow cytometry for the presence of CFSE-labeled OT-II CD4⁺ T cells using antibodies against TCR β , CD4 and CD8 α .

Molecular Fate mapping

CD8 $\alpha\alpha$ T_{unc} or CD8 T_{con} (1×10^5 /well) from livers of PLZF-Cre x R26T (PCre x R26T) and B6 mice were sorted and tdTomato expression was analyzed by FACS.

Cytokines

Sorted CD8 $\alpha\alpha$ T_{unc} or CD8 T_{con} from livers of naïve B6 mice (1×10^5 cells/well) were cultured in 200 μ l of RPMI 1640 medium, 5% FBS, 1% Penicillin/Streptomycin, 2 mM L-glutamine, 25 mM Hepes, 1 \times non-essential amino acids and 1 mM sodium pyruvate (all from Hyclone) plus 50 μ M β -mercaptoethanol and stimulated with anti-CD3 (1 μ g/ml, 145–2C11, BD)-coated plates for 24, 48, 72 and 96 h. Cell culture supernatants were collected at different time points and analyzed for cytokines secretion using BDTM Cytometric Bead Array following the manufactures instructions.

RNA, cDNA synthesis, RT-PCR and Quantitative RT-PCR

CD8 $\alpha\alpha$ T_{unc} or CD8 T_{con} isolated by FACS from liver MNCs were used for RNA isolation. RNA was isolated using the RNeasy mini kit (Qiagen) and quantified using NanoDrop

2000c spectrophotometer (Thermo Scientific). cDNA synthesis was performed using the Reverse Transcription System (Promega). TCR V α usage was performed by PCR using a panel of V α specific oligonucleotide primers and a common C α primer (23). Amplification products were analyzed by electrophoresis in an Ethidium bromide containing 1.5% agarose gel. qPCR were carried out using the Brilliant SYBER Green quantitative PCR kit (Stratagene) on a Stratagene Mx3000P machine (Agilent Technologies). Each PCR contained 2 μ l of cDNA, 25 μ l of 2X Brilliant SYBR Green QPCR Master Mix (Stratagene), 1 μ l of forward and reverse primers (10 μ mol/l), 0.75 μ l of ROX Reference Dye (Stratagene), and 20.25 μ l of sterile water. A typical cycle was as follows: 95°C for 11 min and 40 cycles of 95°C for 45 s, 60°C for 45 s and 72°C for 45 s. Fold change in expression was determined by the 2^{-CT} method. The results were standardized to the mRNA level of β -actin. Data are presented as mRNA fold change against CD8 T_{con}.

High-throughput sequencing of the TCR genes

The TCR β CDR3 regions were amplified and sequenced from sorted CD8 $\alpha\alpha$ T_{unc} and CD8 T_{con} from liver MNCs of naïve B6 mice or from human PBMC. Amplification and sequencing of TCR β CDR3 regions were performed on the ImmunoSEQ platform at Adaptive Biotechnologies (Seattle, WA) as previously described (24). Sequences that did not match CDR3 sequences were removed from the analysis. A standard algorithm was used to identify which V, D, and J segments contributed to each TCR β CDR3 sequence.

Statistics

Data were analyzed using GraphPad Prism v7 software (GraphPad Software). Data are reported as Mean \pm SEM. The two-tailed unpaired t-test, Student's *t* test or Mann Whitney *U* test were used when comparing two groups of unpaired data. The one-way analysis of variance (ANOVA) with Bonferroni's multiple comparisons posttest was used when comparing three or more groups. A paired t test was used when comparing two groups of paired data. Significance was assessed using two-tailed tests and indicated as follow: *P < 0.05, **P < 0.01, ***P < 0.001 and ****P < 0.0001.

Results

CD8 $\alpha\alpha$ T_{unc} are unconventional lymphocytes that form part of the natural repertoire in naïve mice and dependent upon the PLZF transcription factor

The tolerant nature of the hepatic immune system and the expression of CD8 $\alpha\alpha$ homodimers in peptide-induced regulatory CD8⁺ T cell clones in H-2^u mice (9) prompted us to investigate whether CD8 Treg may be enriched in liver of naïve B6 mice. Following the gating strategy in Fig. 1A, we found that around 4% of hepatic TCR $\alpha\beta$ ⁺CD8⁺ T cells are CD8 $\alpha\alpha$ ⁺ and display an activated, innate-like, memory phenotype (CD44^{hi}CD62L^{lo}NK1.1⁺CD69⁺) (Fig. 1B and C). These cells, referred hereafter as CD8 $\alpha\alpha$ T_{unc}, are enriched in the liver of naïve mice, but also present in other peripheral lymphoid organs, including lung, PBMC and spleen (Fig. S1A). Notably, CD8 $\alpha\alpha$ T_{unc} are not detectable in adult thymus (Fig. S1A), but they are present in neonatal thymus until day 5 after birth (Fig. S1B). They are deficient in athymic nude mice (Fig. S1C), indicating their thymic origin. CD8 $\alpha\alpha$ T_{unc} express only the CD8 α but not CD8 β chain as shown by the

loss of CD8 β transcripts in CD8 $\alpha\alpha$ T_{unc} by quantitative PCR (qPCR) and also by their absence in CD8 α ^{-/-} mice (Fig. 1D).

Since innate-like features in T cells are driven by the expression of PLZF transcription factor, also known as Zbtb16 (25, 26), we examined its expression in CD8 $\alpha\alpha$ T_{unc}. Staining of liver MNCs with anti-PLZF mAb in B6 mice and GFP expression in PLZF-eGFP (PEG) reporter mice (27) show that CD8 $\alpha\alpha$ T_{unc} express PLZF, but at levels lower than the invariant NKT (iNKT) cells (Fig. 1E). In contrast, conventional TCR $\alpha\beta$ ⁺CD8 $\alpha\beta$ ⁺ (CD8 T_{con}) or CD4 T cells did not express PLZF (Fig. 1E). The qPCR analysis confirmed that PLZF transcripts are found exclusively in sorted CD8 $\alpha\alpha$ T_{unc} but not in CD8 T_{con} (Fig. 1F). To determine whether CD8 $\alpha\alpha$ T_{unc} expressed PLZF at previous developmental stages, we performed a fate-mapping experiment using PLZF-Cre x R26T (PCre x R26T) mice, in which PLZF-expressing cells are permanently labeled as tdTomato positive cells (27). As shown in Fig. 1G, most hepatic CD8 $\alpha\alpha$ T_{unc} in PCre x R26T mice are tdTomato positive, while CD8 T_{con} show only background level expression. Collectively, these data confirm the expression of PLZF in CD8 $\alpha\alpha$ T_{unc} but not in CD8_{con}.

Next, we compared by qPCR the expression of other transcription factors associated with either innate or activated/memory T cells between sorted CD8 $\alpha\alpha$ T_{unc} and CD8 T_{con}. As shown in Fig. 1H, CD8 $\alpha\alpha$ T_{unc} show up-regulation of *ROR α* (retinoic acid-receptor-related orphan receptor alpha), *Id3* (DNA-binding protein inhibitor ID-3) and *E2A* (immunoglobulin enhancer-binding factors E12/E47) whereas *Id2* (DNA-binding protein inhibitor ID-2), *Eomes* (Eomesodermin) and *HEB* (HeLa E-box binding protein) are down-regulated in comparison to CD8 T_{con}. However, *T-bet* and *KLF2* (Kruppel-like factor 2) expression are not significantly different between CD8 $\alpha\alpha$ T_{unc} and CD8 T_{con}. A critical role of *PLZF* in the development or survival of CD8 $\alpha\alpha$ T_{unc} is shown in *PLZF*^{-/-} mice that have a significantly reduced number of hepatic CD8 $\alpha\alpha$ T_{unc} (Fig. 1I).

CD8 $\alpha\alpha$ T_{unc} secrete cytokines typical of innate-like cytotoxic T cells and use a perforin-dependent mechanism to control autoimmunity

Next, we determined whether hepatic CD8 $\alpha\alpha$ T_{unc} have effector or regulatory function. We analyzed the ability of adoptively transferred CD8 $\alpha\alpha$ T_{unc} to influence myelin-oligodendrocyte glycoprotein (MOG)₃₅₋₅₅-induced experimental autoimmune encephalomyelitis (EAE). Thus, sorted hepatic CD8 $\alpha\alpha$ T_{unc} or CD8 T_{con} from naïve B6 mice were adoptively transferred into B6 recipient mice one day before MOG₃₅₋₅₅-induced EAE. As shown in Fig. 2A, mice that received CD8 $\alpha\alpha$ T_{unc} show a significant suppression of EAE in comparison to those receiving CD8 T_{con} or control mice. Next, to exclude the potential role of both PLZF⁺CD1d-restricted NKT cells as well as innate-like memory CD8⁺ T cells that depend on IL-4 secreted by NKT cells (28), hepatic CD8 $\alpha\alpha$ T_{unc} or CD8 T_{con} were sorted from CD1d^{-/-} mice, which are deficient in both populations, and adoptively transferred into B6 recipients, in which EAE was induced as above. As shown in Fig. 2B, mice that received CD8 $\alpha\alpha$ T_{unc} but not CD8 T_{con} from CD1d^{-/-} mice show significant protection from EAE, indicating that the protective effect of CD8 $\alpha\alpha$ T_{unc} is independent of NKT or NKT-dependent innate-like CD8⁺ T cells. These data indicate that CD8 $\alpha\alpha$ T_{unc} have regulatory properties and inhibit autoimmune T cell responses.

We next investigated whether CD8 $\alpha\alpha$ T_{unc} are expanded *in vivo* due to an autoimmune T cell response. B6 mice were immunized with either MOG_{35–55} peptide or an irrelevant peptide from hen egg lysozyme (HEL)_{74–90} and the frequency of CD8 $\alpha\alpha$ T_{unc} was determined at day 10 (onset of disease, EAE d10) or at day 25 (recovery phase, EAE d25). As shown in Fig. 2C, CD8 $\alpha\alpha$ T_{unc} transiently decrease at the onset of disease but significantly expand during the recovery phase of EAE. In contrast, CD8 $\alpha\alpha$ T_{unc} are not altered in non-diseased HEL-immunized mice. Next, we determined whether the increased frequency of CD8 $\alpha\alpha$ T_{unc} is related to the clinical disease. Interestingly, the frequency of CD8 $\alpha\alpha$ T_{unc} increase significantly in mice that contracted less severe disease (scores 0–1) in comparison to those with more severe disease (scores 3–4) (Fig. 2D), suggesting their involvement in the control of EAE as suggested earlier for CD8 T cells (7–10, 29). These data indicate that regulatory CD8 $\alpha\alpha$ T_{unc} are expanded following an autoimmune inflammatory response.

To investigate whether CD8 $\alpha\alpha$ T_{unc} can control autoimmunity in the absence of other Treg, we used the CD4⁺CD45RB^{hi} T cell transfer model of colitis in Rag1^{–/–} mice. Since regulatory CD8⁺ T cells has been shown to use perforin to kill activated effector T cells (10, 30), Rag1^{–/–} mice were co-transferred with CD4⁺CD25[–]CD45RB^{hi} T cells along with sorted CD8 $\alpha\alpha$ T_{unc} either from B6 (perforin^{+/+}) or perforin^{–/–} mice. As shown in Fig. 2E, Rag1^{–/–} recipients that received CD8 $\alpha\alpha$ T_{unc} from perforin^{–/–} mice develop colitis similar to that in control mice. In contrast, those receiving CD8 $\alpha\alpha$ T_{unc} from B6 (perforin^{+/+}) mice are significantly protected from disease as indicated by an increased BW ratio and amelioration of colonic inflammation as shown by H&E staining. These results indicate that the perforin pathway is an important cytotoxic mechanism used by CD8 $\alpha\alpha$ T_{unc} to control autoimmunity mediated by activated CD4⁺ T cells.

Next, to determine whether CD8 $\alpha\alpha$ T_{unc} can also control *in vivo* activated CD4⁺ T cells reactive to a foreign antigen, we analyzed their capacity from B6 (perforin^{+/+}) or perforin^{–/–} mice to suppress the anti-OVA CD4 T cell response. As shown in Fig. 2F and Fig. S2, CD8⁺ T cells from B6 but not from perforin^{–/–} mice significantly suppress activated CD4⁺ T cells as indicated by a significantly reduced proliferation and recovery of CFSE-labeled OT-II CD4 T cells in the presence of functional CD8⁺ T cells. Consistent with the *in vivo* data, sorted hepatic CD8 $\alpha\alpha$ T_{unc} but not CD8 T_{con} also inhibit *in vitro* proliferation of anti-CD3 activated CFSE-labeled polyclonal CD4⁺ T cells (Fig. 2G).

Next, to investigate whether suppressive cytokines may also be involved in regulation, we determined the cytokine secretion profile of sorted hepatic CD8 $\alpha\alpha$ T_{unc} from naïve B6 following *in vitro* stimulation with plate-bound anti-CD3 mAb. As shown in Fig. 3, CD8 $\alpha\alpha$ T_{unc} secrete typical pro-inflammatory cytokines produced by innate-like cytotoxic T cells (TNF α , IL-17A and IL-6) as well as IFN γ and IL-4. In contrast, hepatic CD8 T_{con} show a typical cytotoxic T cell profile and do not secrete IL-4 and IL-17A. Notably, CD8 $\alpha\alpha$ T_{unc} secrete significantly higher levels of IL-2 within 24 h, while CD8 T_{con} secrete only a minimal amount (Fig. 3). Importantly, CD8 $\alpha\alpha$ T_{unc} do not secrete the suppressive cytokine IL-10 (Fig. 3) and do not express TGF β (Fig. 5E). Thus, CD8 $\alpha\alpha$ T_{unc} secrete cytokines typical of innate-like cytotoxic T cells and not suppressive cytokines.

Innate-like CD8 $\alpha\alpha$ T_{unc} are polyclonal and use diverse TCR α and β chains

Since PLZF-dependent innate-like T cells often use limited TCR repertoires (4), we determined the TCR repertoire of hepatic CD8 $\alpha\alpha$ T_{unc}. As shown in Fig. 4A, the TCR V β repertoire of sorted CD8 $\alpha\alpha$ T_{unc} is diverse with a bias toward the use of V β 8.1/8.2, V β 5.1/5.2 and V β 11 chains, similar to the CD8 T_{con}. Next, the TCR β repertoire of sorted hepatic CD8 $\alpha\alpha$ T_{unc} and CD8 T_{con} was analyzed by high-throughput sequencing as described before (24). A total of 665 and 98,935 productive TCR β sequences were obtained from CD8 $\alpha\alpha$ T_{unc} and CD8 T_{con}, respectively. From these, 31 and 7,256 unique TCR β clonotypes at the CDR3 amino acid level were assembled from CD8 $\alpha\alpha$ T_{unc} and CD8 T_{con}, respectively. Consistent with the flow cytometric analysis, CD8 $\alpha\alpha$ T_{unc} express a diverse TCR β repertoire with a preferential usage of TRBV13-3/13-2 (V β 8.1/8.2), TRBV20 (V β 15), TRBV12-1/12-2 (V β 5.1/5.2), TRBV5 (V β 1) and TRBV4 (V β 10) (Fig. 4B). Additionally, TRBJ usage, another indicator of the heterogeneity, is also diverse and almost similar among CD8 $\alpha\alpha$ T_{unc} and CD8 T_{con}, except for an increase in J β 2.5 usage by CD8 $\alpha\alpha$ T_{unc} (Fig. S3A, left). CD8 $\alpha\alpha$ T_{unc} also show a slightly skewed bell-shaped distribution of CDR3 lengths with a peak at 39 nt, while CD8 T_{con} show a more typical Gaussian-like distribution with a peak at 42 nt (Fig. S3A, right). Furthermore, TCR V α analysis of CD8 $\alpha\alpha$ T_{unc} by flow cytometry (Fig. 4C) and RT-PCR (Fig. 4D) reveal a diverse V α usage similar to that in CD8 T_{con}.

CD8 $\alpha\alpha$ T_{unc} are dependent on IL-15/IL-2R β for their development/survival and express several immune regulatory receptors

We next determined the cytokine and cytokine signaling requirement for the development or survival of CD8 $\alpha\alpha$ T_{unc}. Since CD122 or the IL-2R β chain has been shown to be essential for IL-15 signaling, we first investigated the role of IL-15. As shown in Fig. 5A, CD8 $\alpha\alpha$ T_{unc} are dramatically reduced in both CD122^{-/-} and IL-15^{-/-} mice in comparison to B6 mice. In contrast, CD8 $\alpha\alpha$ T_{unc} are not affected in CD25^{-/-}, IL-7^{-/-}, IL-6^{-/-} and IFN γ ^{-/-} mice. Surprisingly, unlike NKT cells, CD8 $\alpha\alpha$ T_{unc} are not reduced in T-bet^{-/-} mice (Fig. 5A). Furthermore, no significant changes in the frequency of hepatic CD8 $\alpha\alpha$ T_{unc} are observed in CD1d^{-/-} and Ja.18^{-/-}, indicating their distinctiveness from NKT cells and that CD1d or NKT cells are not required for CD8 $\alpha\alpha$ T_{unc} development (Fig. 5A). Furthermore, the presence of CD8 $\alpha\alpha$ T_{unc} in MR1^{-/-}, μ MT^{-/-} (Fig. 5A) as well as in germ-free mice (Fig. 1SD) indicates their phenotype being distinct from the MAIT cells.

Since CD8 $\alpha\alpha$ T_{unc} have regulatory activity, we analyzed the expression of several markers associated with regulatory function. CD8 $\alpha\alpha$ T_{unc} do not express FoxP3 but do express glucocorticoid-induced tumor necrosis factor-related receptor (GITR) (Fig. 5B). As shown in Fig. 5C, CD8 $\alpha\alpha$ T_{unc} are CD25^{lo}, CD122^{hi}, are not typical memory T cells as they do not express CD127 and are IL-7-independent (Fig. 5A). Higher expression of CD122 in CD8 $\alpha\alpha$ T_{unc} and their absence in IL-15^{-/-} mice is consistent with the requirement for IL-15 for their survival/development. Interestingly, CD8 $\alpha\alpha$ T_{unc} express PD-1⁺ (~25%) CD28⁺ (~44%), CD27^{hi} (~72%) and CD200 (~35%), a negative signaling molecule (Fig. 5C). In addition, CD8 $\alpha\alpha$ T_{unc} did not express OX-40, ICOS, CXCR5, Eomes and CD103 (Fig. 5C) (31). Importantly, CD8 $\alpha\alpha$ T_{unc} express only NK inhibitory receptors (Ly49E/

F>Ly49G2>Ly49A>Ly49I>Ly49G) but not activating receptors (Ly49D and Ly49H) (Fig. 5D).

Next, to further confirm their phenotype, we analyzed the expression of several genes in sorted hepatic CD8 $\alpha\alpha$ T_{unc} by qPCR. Consistent with the flow cytometry data, CD8 $\alpha\alpha$ T_{unc} show significant up-regulation of *CD28*, *CD122*, *Ly49A* and *CD200* (Fig. 5E). Furthermore, CD8 $\alpha\alpha$ T_{unc} greatly up-regulated *2B4* (CD244), *Gzma* (Granzyme A), *Light* and chemokine receptors, including *Cxcr3*, *Gpr15* and *Ccr5*. Interestingly, *Fgl2* (Fibrinogen-like 2), which is also a negative regulator of the immune response, is up-regulated in CD8 $\alpha\alpha$ T_{unc}. In contrast, other genes associated with CD4 Treg, including *TGF- β 1* and *LAG-3* (Lymphocyte-activation gene 3), are down-regulated in comparison to CD8 T_{con} (Fig. 5E).

Co-expression of CD11c and CD244 distinguishes a functionally distinct population within the heterogeneous CD8 $\alpha\alpha$ T_{unc}

Further, we determined the expression of other cell surface markers associated with immune regulation within the polyclonal CD8 $\alpha\alpha$ T_{unc} population. We found that a large portion (~40–50%) of hepatic CD8 $\alpha\alpha$ T_{unc} in naïve mice co-express CD11c and CD244 and that all CD11c⁺ cells are CD244⁺ (Fig. 6A). In contrast, hepatic CD8 T_{con} express negligible levels of CD11c or CD244 (Fig. 6A). Interestingly, CD244 is a NK cell marker associated with inhibitory receptor function (32) and CD11c has also been shown to be expressed on splenic suppressor CD8⁺ T cells (18). As expected, CD244⁺CD11c⁺ CD8 $\alpha\alpha$ T_{unc} are significantly reduced in PLZF^{-/-} mice (Fig. 6B) and also express NK1.1 and NKG2D (Fig. 6C). Using PEG mice, we further confirmed that CD244⁺CD11c⁺ CD8 $\alpha\alpha$ T_{unc} are PLZF⁺ and express higher levels of PLZF in comparison to CD244⁻CD11c⁻ cells (Fig. 6D).

To determine whether the CD11c expression in CD8 $\alpha\alpha$ T_{unc} identify a functionally different population, sorted CD8 $\alpha\alpha$ T_{unc} depleted of CD11c⁺ cells (CD8 $\alpha\alpha$ ⁺CD11c⁻ cells) were adoptively transferred into naïve B6 recipients to examine their ability to control EAE as in Fig. 2A. As shown in Fig. 6E, adoptive transfer of CD8 $\alpha\alpha$ ⁺CD11c⁻ cells did not protect recipient mice from MOG_{35–55}-induced EAE, suggesting that the loss of CD11c⁺ cells within the polyclonal CD8 $\alpha\alpha$ T_{unc} population results in loss of their regulatory capacity.

Since unconventional T cells are restricted by MHC Class Ib molecules and the Qa-1^b molecule has been suggested to be involved in immune regulation (9, 10, 29), we determined the frequency of hepatic CD8 $\alpha\alpha$ T_{unc} in Qa-1^b^{-/-} mice. As shown in Fig. 6F and 6G, CD8 $\alpha\alpha$ T_{unc} populations are significantly reduced in Qa-1^b^{-/-} mice, indicating that a proportion of CD8 $\alpha\alpha$ T_{unc} are Qa-1^b-restricted. Since Qa-1^b-restricted T cells can be either TAP-dependent or TAP-independent, we also examined the frequency of CD8 $\alpha\alpha$ T_{unc} in TAP1^{-/-} mice. As shown in Fig. 6F, the frequency of CD8 $\alpha\alpha$ T_{unc} is not different between TAP1^{-/-} and B6 mice, indicating that TAP-dependent antigen processing is not required for the development of these cells.

PLZF⁺CD161^{int/lo} CD8 $\alpha\alpha$ T_{unc} are present in human PBMC and are polyclonal

To identify a human counterpart to the murine CD8 $\alpha\alpha$ T_{unc}, we determined their presence in PBMC from healthy subjects. Gating strategy (Fig. 7A) is based on PLZF expression in TCR $\alpha\beta$ ⁺CD8⁺ T cells and exclusion of CD8 β ⁺ T cells as well as CD8 $\alpha\alpha$ ⁺ MAIT cells (33).

Therefore, CD8 $\alpha\alpha$ T_{unc} in humans are identified as TCR $\alpha\beta$ ⁺PLZF⁺CD8 β ⁻CD8 $\alpha\alpha$ ⁺CD161^{int/lo} and represent ~ 11.9% \pm SEM 2.1 in PBMC (Fig. 7B) and 0.25% \pm 0.06 and 0.92% \pm 0.22 in total TCR $\alpha\beta$ ⁺ T cells and CD8⁺ T cells, respectively. In contrast, MAIT cells represent 2.6% \pm 0.54 of the total TCR $\alpha\beta$ ⁺ T cells and 9% \pm 1.9 of the CD8⁺ T cells. Next, we determined the expression of various immune markers as well as cytokines in human CD8 $\alpha\alpha$ T_{unc} directly *ex vivo* without stimulation and compared them with MAIT cells and CD8 T_{con}. Human CD8 $\alpha\alpha$ T_{unc} are composed mainly of memory populations (~50% CCR7⁻CD45RA⁺ T_{EMRA} and ~30% CCR7⁻CD45RA⁻ T_{EM} cells) and more than 80% of CD244⁺CD11c⁺ CD8 $\alpha\alpha$ T_{unc} are T_{EMRA} cells (Fig. 7C). Similarly, human CD8 $\alpha\alpha$ T_{unc} express higher levels of CD244, CD11c and granzyme B in comparison to CD8 T_{con} and MAIT cells (Fig. 7D). Furthermore, the expression of markers known to be up-regulated in MAIT cells, including IL-18R α 1, ROR γ t, CXCR6 and CCR6, is significantly reduced in CD8 $\alpha\alpha$ T_{unc} (Fig. S4). Similar to murine, human CD8 $\alpha\alpha$ T_{unc} also secrete IFN γ , IL-17A, TNF α and IL-4 (Fig. S4). Importantly, a substantial portion (~17%) of human CD8 $\alpha\alpha$ T_{unc} but not MAIT cells are CD244⁺CD11c⁺ (Fig. 7E) and the majority of human CD244⁺CD11c⁺ CD8 $\alpha\alpha$ T_{unc} secrete both Granzyme B and perforin (Fig. 7F).

Next, the TCR β repertoire of sorted CD8 $\alpha\alpha$ T_{unc} and CD8 T_{con} was analyzed by high-throughput sequencing as described before (24). A total of 73,760 and 386,832 productive TCR β sequences were obtained from CD8 $\alpha\alpha$ T_{unc} and CD8 T_{con}, respectively. From these, 794 and 12,244 unique TCR β clonotypes at the CDR3 amino acid level were assembled from CD8 $\alpha\alpha$ T_{unc} and CD8 T_{con}, respectively. Similar to murine cells, human CD8 $\alpha\alpha$ T_{unc} exhibit a non-restricted usage of multiple TRBV gene segments resembling the TCR β repertoire of CD8 T_{con} (Fig. 7G). Also, they do not show any preferential usage of specific TRBJ gene segment (Fig. S3B, left) and show a Gaussian-like CDR3 β length distribution profiles (Fig. S3B, right).

Discussion

The immune tolerance function of liver has been known for long time, but the cellular and molecular mechanism(s) mediating regulation are poorly understood. Here, we have identified and characterized a novel population of unconventional, innate-like TCR $\alpha\beta$ ⁺CD8 $\alpha\alpha$ ⁺ T cells, named as CD8 $\alpha\alpha$ T_{unc}, enriched in liver of naïve mice and capable of regulating autoimmune responses. Their importance is further highlighted by the fact that these polyclonal cells are also present as part of the natural immune repertoire in humans.

The expression of the PLZF transcription factor in CD8 $\alpha\alpha$ T_{unc} in both mice and humans distinguishes them from conventional CD8 $\alpha\beta$ T cells. PLZF expression also confers innate-like characteristics in hepatic CD8 $\alpha\alpha$ T_{unc}, including expression of activation, memory and NK cell markers similar to those in NKT cells (25, 26), thus, allowing them to act promptly. Unlike the Foxp3, PLZF expression is not inducible in conventional T cells following activation (27). Therefore, CD8 $\alpha\alpha$ T_{unc} represent a separate lineage of unconventional CD8⁺ T cells distinct from CD8 T_{con}. Consistently, higher expression of PLZF, ROR α (34) and Id3 (35) and significantly reduced numbers of CD8 $\alpha\alpha$ T_{unc} in mice genetically deficient in PLZF^{-/-} mice as well as in ROR α - and Id3-deficient mice (data not shown) suggests a differential transcription requirement for the development of CD8 $\alpha\alpha$ T_{unc}. The down-

regulation of the transcriptional repressor Id2 (DNA-binding protein inhibitor ID-2) (36) also indicates that CD8 $\alpha\alpha$ T_{unc} belong to a T cell lineage rather than to an innate lymphoid lineage.

Though, hepatic CD8 $\alpha\alpha$ T_{unc} share several characteristics with other innate-like unconventional T cells, such as NKT and MAIT cells, they have several distinguishing features: (a) CD8 $\alpha\alpha$ T_{unc} are present in liver of both CD1d^{-/-} and Ja18^{-/-} mice, therefore, they are not CD1d-restricted and they are distinct from other NKT-dependent innate-like CD8⁺ T cells (28); (b) unlike MAIT cells, CD8 $\alpha\alpha$ T_{unc} are present in MR1^{-/-}, germ-free mice and in B cell-deficient mice; (c) presence of CD8 $\alpha\alpha$ T_{unc} in CD1d^{-/-}, MR1^{-/-} and germ-free mice indicates that these cells are not reactive to lipid and the commensal bacterial antigens, respectively; (d) distinct from the semi-invariant TCR repertoire of MAIT or iNKT cells, the TCR α and β repertoire of CD8 $\alpha\alpha$ T_{unc} is highly diverse; (e) while CD8 $\alpha\alpha$ T_{unc} do not express ICOS, CD127 and CD103, MAIT cells are positive for expression of these markers; (f) MAIT cells do not secrete IL-2 while CD8 $\alpha\alpha$ T_{unc} promptly secrete large amount of IL-2 following stimulation; (g) different from MAIT cells, human CD8 $\alpha\alpha$ T_{unc} have lower expression of CD161 and significantly lower levels of IL-18R α , CXCR6, CCR6 and ROR γ t; and (h) CD8 $\alpha\alpha$ T_{unc} co-express CD11c and CD244 and secrete higher levels of both granzyme B and perforin.

One of the important features of hepatic CD8 $\alpha\alpha$ T_{unc} is that they are immunoregulatory and can control autoimmune T cell responses mediating EAE as well as colitis. The ability of adoptively transferred CD8 $\alpha\alpha$ T_{unc} to suppress colitis in Rag1^{-/-} mice in a perforin-dependent manner further indicates that these cells use cytotoxic mechanisms to kill activated effector CD4⁺ T cells to regulate autoimmunity, independently of other Treg, as shown earlier for Qa-1-restricted CD8⁺ regulatory T cells (10, 30). Interestingly, perforin/granzyme cytotoxic pathway has also been shown to be used by natural FoxP3⁺CD4⁺ Treg to kill effector T cells (37). Since, CD8 $\alpha\alpha$ T_{unc} could be restricted by class I^a or class I^b MHC molecules, reviewed in (38), a significant loss of CD8 $\alpha\alpha$ T_{unc} in Qa-1^b-deficient mice indicate that a substantial number of these cells are non-classical class I^b MHC-restricted. Because naïve T cells are Qa-1^b-negative, only activated T cells that are Qa-1^b-positive are targets of CD8 $\alpha\alpha$ T_{unc}-mediated cytotoxic mechanisms (9, 10, 39). Furthermore, CD8 $\alpha\alpha$ T_{unc} do not secrete IL-10 and TGF β , therefore, additional suppressive mechanisms, including anergy (40) or indoleamine 2,3-dioxygenase (41) pathways, may also be used. Enrichment of CD8 $\alpha\alpha$ T_{unc} during the recovery phase of EAE suggests that an ongoing pro-inflammatory, chronic autoimmune response triggers expansion of these Treg, as suggested earlier (9, 10). Another important feature of CD8 $\alpha\alpha$ T_{unc} is their ability to rapidly secrete large amount of IL-2 that may be relevant not only for the maintenance of their memory phenotype (42), but also for the expansion/survival of Foxp3⁺CD4⁺ Treg in the liver.

CD4⁺ Treg constitutively express CD25, a high affinity IL-2R (43) and CD25 deficiency in both mice and humans results in the loss of peripheral tolerance due to reduced CD4⁺ Treg (44, 45). In contrast, CD8 $\alpha\alpha$ T_{unc} express higher levels of CD122 or IL-2R β and they are lost in CD122^{-/-} but not in CD25^{-/-} mice. Furthermore, IL-2R β -deficient mice also develop severe autoimmunity, splenomegaly and elevated autoantibodies and can be rescued by adoptive transfer of either CD122⁺CD8⁺ T cells (19) or CD4⁺ Treg (46) from naïve mice.

Recently, IL-2R β mutations in humans also have been shown to result in loss of peripheral tolerance, multisystem autoimmunity and CMV disease (47, 48). Additionally, genome-wide association studies have implicated IL-2R β -mediated signaling in human autoimmune diseases (49, 50). Thus, studies in both mice and humans suggest that regulatory T cell-mediated immune tolerance is focused on IL-2R signaling: IL-2R α for the CD4⁺ Treg and IL-2R β for CD8 $\alpha\alpha$ T_{unc}.

Hepatic CD8 $\alpha\alpha$ T_{unc} express an activated/memory phenotype (CD69⁺CD44^{hi}CD62^{lo}) as shown for other CD8⁺ tissue-resident memory T cells (51, 52). However, they do not express CD103, an important integrin for T cell residence in epithelial tissues. It is likely that, similar to iNKT cells, CD8 $\alpha\alpha$ T_{unc} use PLZF-driven up-regulation of LFA-ICAM-1 interactions for retention in liver (53). Consistent with their activated memory phenotype, IL-15 signaling is critical for the development or survival of CD8 $\alpha\alpha$ T_{unc} as they are significantly depleted in liver of mice deficient in IL-15. A constitutive production of IL-15 in liver (54) may provide a suitable environment for their development or survival. In fact, neonatal liver is significantly enriched in CD8 $\alpha\alpha$ T_{unc} while these cells are undetectable in thymus 5 days after birth. Absence of CD8 $\alpha\alpha$ T_{unc} in thymectomized mice suggest thymic dependence for their development as shown earlier for thymic and intestinal CD8 $\alpha\alpha$ T cells (55, 56). It is possible that CD8 $\alpha\alpha$ T_{unc} may migrate into liver to fully differentiate as shown for intestinal CD8 $\alpha\alpha$ T cells (56). A polyclonal TCR repertoire and an activated phenotype of hepatic CD8 $\alpha\alpha$ T_{unc} also suggest that these cells recognize diverse self-antigens as part of the homeostatic mechanism in naïve mice. Homeostatic expansion of CD8 $\alpha\alpha$ T_{unc} may depend on the type I IFN receptor signaling pathway required for the IL-15 production (57). Accordingly, STAT-1, which is essential for type I IFN receptor signaling (58), may also be important for CD8 $\alpha\alpha$ T_{unc} survival. Consistently, STAT-1^{-/-} but not STAT-2^{-/-} mice have normal repertoire of CD8 T_{con} but lack Ly49⁺ CD8⁺ T cells and develop massive infiltration of CD4⁺ T cells into liver (59).

The presence of CD8 $\alpha\alpha$ T_{unc} in naïve mice and in PBMC of healthy subjects suggests that these cells are part of the natural immune repertoire. The TCR repertoire and phenotypic analysis indicate that CD8 $\alpha\alpha$ T_{unc} are polyclonal, similar to innate-like type II NKT cells (60) and express cell surface molecules that have been shown to be present in peripherally induced regulatory CD8⁺ T cells, including Ly49, CD11c and PD-1 (9, 16-19). Thus, CD8 $\alpha\alpha$ T_{unc} are comprised of functionally distinct populations, including regulatory CD11c⁺CD244⁺ CD8 $\alpha\alpha$ T_{unc} present in both mice and humans. These cells also secrete increased levels of perforin and granzyme B in humans in steady state. Interestingly, CD137-induced CD8⁺CD11c⁺ T cells have been shown to suppress autoimmune diseases (18). Recently, TCR $\alpha\beta$ ⁺CD8⁺CD11c⁺ T cells with DC properties have been also described in mice and humans (61), but differ from CD8 $\alpha\alpha$ T_{unc} in that they are CD127^{hi} and negative for CD69, CD25, CD122, NK1.1 and PLZF expression. CD8 $\alpha\alpha$ T_{unc} also express NKG2D and Ly49 NK-inhibitory receptors shown to be expressed by Qa-1-restricted regulatory CD8⁺ T cells (16, 17). Hepatic PD1⁺CD8⁺ T cells have recently been shown to promote efficient tolerance toward a fully allogeneic graft (62). Although, we have not analyzed CD8 $\alpha\alpha$ T_{unc} in human liver, recent reports indicate an enrichment of memory CD8⁺ T cells with similar features, for example, IL-2-secreting PD1⁺CD69⁺CD103⁻CD8⁺ (42) and granzyme-secreting CD161^{int}CD8⁺ T cells (42, 63, 64). Also, loss of a terminally differentiated regulatory CD8⁺

T cell population in multiple sclerosis patients with clinical disease exacerbation has been shown (65). Since, CD8 $\alpha\alpha$ T_{unc} are polyclonal and have different MHC restrictions, it is possible that they may also participate in effector functions as recently shown for unconventional CD8⁺ T cells against parasitic (66), SIV (67) and bacterial infections (68). Thus, further molecular and functional studies are needed to identify different subsets of CD8 $\alpha\alpha$ T_{unc}, similar to the presence of multiple functional regulatory and non-regulatory subsets found within the FoxP3⁺CD4⁺ T cells in humans (5).

In summary, we have identified a natural and unique unconventional TCR $\alpha\beta$ ⁺CD8 $\alpha\alpha$ ⁺ T cell population in both mice and humans with potent immune regulatory properties. Our studies significantly contribute to the importance of the emerging diversity of unconventional T cells and their important role in the regulation of autoimmune and inflammatory diseases.

Supplementary Material

Refer to Web version on PubMed Central for supplementary material.

Acknowledgements

This work was started at the Torrey Pines Institute for Molecular Studies and has been performed with the support of the Flow Cytometry Core at the UC San Diego Center for AIDS Research, the VA San Diego Health Care System, and the San Diego Veterans Medical Research Foundation.

This work was supported by National Institutes of Health Grants R01 AI052227 to VK.

Abbreviations used in this article:

B6	C57BL/6
EAE	Experimental Autoimmune Encephalomyelitis
Eomes	Eomesodermin
GITR	glucocorticoid-induced tumor necrosis factor-related receptor
HEL	hen egg lysozyme
Id3	DNA-binding protein inhibitor ID-3
MOG	myelin-oligodendrocyte glycoprotein
NKT	natural killer T cells
MAIT	mucosal-associated invariant T cells
MNCs	mononuclear cells
PBMC	peripheral blood mononuclear cells
PLZF	promyelocytic leukemia zinc finger
qPCR	quantitative PCR

ROR α retinoic acid-receptor-related orphan receptor alpha**References**

1. Calne RY, Sells RA, Pena JR, Davis DR, Millard PR, Herbertson BM, Binns RM, and Davies DA. 1969 Induction of immunological tolerance by porcine liver allografts. *Nature* 223: 472–476. [PubMed: 4894426]
2. Protzer U, Maini MK, and Knolle PA. 2012 Living in the liver: hepatic infections. *Nat Rev Immunol* 12: 201–213. [PubMed: 22362353]
3. Crispe IN 2011 Liver antigen-presenting cells. *J Hepatol* 54: 357–365. [PubMed: 21084131]
4. Godfrey DI, Le Nours J, Andrews DM, Uldrich AP, and Rossjohn J. 2018 Unconventional T Cell Targets for Cancer Immunotherapy. *Immunity* 48: 453–473. [PubMed: 29562195]
5. Wing JB, Tanaka A, and Sakaguchi S. 2019 Human FOXP3(+) Regulatory T Cell Heterogeneity and Function in Autoimmunity and Cancer. *Immunity* 50: 302–316. [PubMed: 30784578]
6. Gershon RK, and Kondo K. 1970 Cell interactions in the induction of tolerance: the role of thymic lymphocytes. *Immunology* 18: 723–737. [PubMed: 4911896]
7. Jiang H, Zhang SI, and Pernis B. 1992 Role of CD8+ T cells in murine experimental allergic encephalomyelitis. *Science* 256: 1213–1215. [PubMed: 1375398]
8. Koh D-R, Fung-Leung W-P, Ho A, Gray D, Acha-Orbea H, and M. TW 1992 Less mortality but more relapses in experimental allergic encephalomyelitis in CD8^{-/-} mice. *Science* 256: 1210–1213. [PubMed: 1589800]
9. Tang X, Maricic I, Purohit N, Bakamjian B, Reed-Loisel LM, Beeston T, Jensen P, and Kumar V. 2006 Regulation of immunity by a novel population of Qa-1-restricted CD8 α alpha+TCR α beta+ T cells. *J Immunol* 177: 7645–7655. [PubMed: 17114434]
10. Hu D, Ikizawa K, Lu L, Sanchirico ME, Shinohara ML, and Cantor H. 2004 Analysis of regulatory CD8 T cells in Qa-1-deficient mice. *Nat Immunol* 5: 516–523. [PubMed: 15098030]
11. Giang S, and La Cava A. 2016 Regulatory T Cells in SLE: Biology and Use in Treatment. *Curr Rheumatol Rep* 18: 67. [PubMed: 27704250]
12. Colovai AI, Mirza M, Vlad G, Wang S, Ho E, Cortesini R, and Suciuc-Foca N. 2003 Regulatory CD8+CD28⁻ T cells in heart transplant recipients. *Hum Immunol* 64: 31–37. [PubMed: 12507812]
13. Brimnes J, Allez M, Dotan I, Shao L, Nakazawa A, and Mayer L. 2005 Defects in CD8+ regulatory T cells in the lamina propria of patients with inflammatory bowel disease. *J Immunol* 174: 5814–5822. [PubMed: 15843585]
14. Zhang J, Medaer R, Stinissen P, Hafler D, and Raus J. 1993 MHC-restricted depletion of human myelin basic protein-reactive T cells by T cell vaccination. *Science* 261: 1451–1454. [PubMed: 7690157]
15. Karandikar NJ, Crawford MP, Yan X, Ratts RB, Brenchley JM, Ambrozak DR, Lovett-Racke AE, Frohman EM, Stastny P, Douek DC, Koup RA, and Racke MK. 2002 Glatiramer acetate (Copaxone) therapy induces CD8(+) T cell responses in patients with multiple sclerosis. *J Clin Invest* 109: 641–649. [PubMed: 11877472]
16. Kim HJ, Wang X, Radfar S, Sproule TJ, Roopenian DC, and Cantor H. 2011 CD8+ T regulatory cells express the Ly49 Class I MHC receptor and are defective in autoimmune prone B6-Yaa mice. *Proc Natl Acad Sci U S A* 108: 2010–2015. [PubMed: 21233417]
17. Fanchiang SS, Cojocaru R, Othman M, Khanna R, Brooks MJ, Smith T, Tang X, Maricic I, Swaroop A, and Kumar V. 2012 Global expression profiling of peripheral Qa-1-restricted CD8 α alpha+TCR α beta+ regulatory T cells reveals innate-like features: implications for immune-regulatory repertoire. *Hum Immunol* 73: 214–222. [PubMed: 21889557]
18. Seo SK, Choi JH, Kim YH, Kang WJ, Park HY, Suh JH, Choi BK, Vinay DS, and Kwon BS. 2004 4-1BB-mediated immunotherapy of rheumatoid arthritis. *Nat Med* 10: 1088–1094. [PubMed: 15448685]
19. Rifa'i M, Kawamoto Y, Nakashima I, and Suzuki H. 2004 Essential roles of CD8+CD122+ regulatory T cells in the maintenance of T cell homeostasis. *J Exp Med* 200: 1123–1134. [PubMed: 15520244]

20. Maricic I, Marrero I, Eguchi A, Nakamura R, Johnson CD, Dasgupta S, Hernandez CD, Nguyen PS, Swafford AD, Knight R, Feldstein AE, Loomba R, and Kumar V. 2018 Differential Activation of Hepatic Invariant NKT Cell Subsets Plays a Key Role in Progression of Nonalcoholic Steatohepatitis. *J Immunol* 201: 3017–3035. [PubMed: 30322964]
21. Jahng A, Maricic I, Aguilera C, Cardell S, Halder RC, and Kumar V. 2004 Prevention of autoimmunity by targeting a distinct, noninvariant CD1d-reactive T cell population reactive to sulfatide. *J Exp Med* 199: 947–957. [PubMed: 15051763]
22. Jahng AW, Maricic I, Pedersen B, Burdin N, Naidenko O, Kronenberg M, Koezuka Y, and Kumar V. 2001 Activation of natural killer T cells potentiates or prevents experimental autoimmune encephalomyelitis. *J Exp Med* 194: 1789–1799. [PubMed: 11748280]
23. Casanova JL, Romero P, Widmann C, Kourilsky P, and Maryanski JL. 1991 T cell receptor genes in a series of class I major histocompatibility complex-restricted cytotoxic T lymphocyte clones specific for a *Plasmodium berghei* nonapeptide: implications for T cell allelic exclusion and antigen-specific repertoire. *J Exp Med* 174: 1371–1383. [PubMed: 1836010]
24. Marrero I, Aguilera C, Hamm DE, Quinn A, and Kumar V. 2016 High-throughput sequencing reveals restricted TCR Vbeta usage and public TCRbeta clonotypes among pancreatic lymph node memory CD4(+) T cells and their involvement in autoimmune diabetes. *Mol Immunol* 74: 82–95. [PubMed: 27161799]
25. Savage AK, Constantinides MG, Han J, Picard D, Martin E, Li B, Lantz O, and Bendelac A. 2008 The transcription factor PLZF directs the effector program of the NKT cell lineage. *Immunity* 29: 391–403. [PubMed: 18703361]
26. Kovalovsky D, Uche OU, Eladad S, Hobbs RM, Yi W, Alonzo E, Chua K, Eidson M, Kim HJ, Im JS, Pandolfi PP, and Sant'Angelo DB. 2008 The BTB-zinc finger transcriptional regulator PLZF controls the development of invariant natural killer T cell effector functions. *Nat Immunol* 9: 1055–1064. [PubMed: 18660811]
27. Zhang S, Laouar A, Denzin LK, and Sant'Angelo DB. 2015 *Zbtb16* (PLZF) is stably suppressed and not inducible in non-innate T cells via T cell receptor-mediated signaling. *Sci Rep* 5: 12113. [PubMed: 26178856]
28. Weinreich MA, Odumade OA, Jameson SC, and Hogquist KA. 2010 T cells expressing the transcription factor PLZF regulate the development of memory-like CD8+ T cells. *Nat Immunol* 11: 709–716. [PubMed: 20601952]
29. Jiang H, Ware R, Stall A, Flaherty L, Chess L, and Pernis B. 1995 Murine CD8+ T cells that specifically delete autologous CD4+ T cells expressing V beta 8 TCR: a role of the Qa-1 molecule. *Immunity* 2: 185–194. [PubMed: 7895175]
30. Beeston T, Smith TR, Maricic I, Tang X, and Kumar V. 2010 Involvement of IFN-gamma and perforin, but not Fas/FasL interactions in regulatory T cell-mediated suppression of experimental autoimmune encephalomyelitis. *J Neuroimmunol* 229: 91–97. [PubMed: 20708278]
31. Ariotti S, Haanen JB, and Schumacher TN. 2012 Behavior and function of tissue-resident memory T cells. *Adv Immunol* 114: 203–216. [PubMed: 22449783]
32. Assarsson E, Kambayashi T, Persson CM, Chambers BJ, and Ljunggren HG. 2005 2B4/CD48-mediated regulation of lymphocyte activation and function. *J Immunol* 175: 2045–2049. [PubMed: 16081768]
33. Fergusson JR, Smith KE, Fleming VM, Rajoriya N, Newell EW, Simmons R, Marchi E, Bjorkander S, Kang YH, Swadling L, Kurioka A, Sahgal N, Lockstone H, Baban D, Freeman GJ, Sverremark-Ekstrom E, Davis MM, Davenport MP, Venturi V, Ussher JE, Willberg CB, and Klenerman P. 2014 CD161 defines a transcriptional and functional phenotype across distinct human T cell lineages. *Cell Rep* 9: 1075–1088. [PubMed: 25437561]
34. Dzhagalov I, Giguere V, and He YW. 2004 Lymphocyte development and function in the absence of retinoic acid-related orphan receptor alpha. *J Immunol* 173: 2952–2959. [PubMed: 15322153]
35. Ji Y, Pos Z, Rao M, Klebanoff CA, Yu Z, Sukumar M, Reger RN, Palmer DC, Borman ZA, Muranski P, Wang E, Schrumph DS, Marincola FM, Restifo NP, and Gattinoni L. 2011 Repression of the DNA-binding inhibitor Id3 by Blimp-1 limits the formation of memory CD8+ T cells. *Nat Immunol* 12: 1230–1237. [PubMed: 22057288]

36. Mjosberg J, Bernink J, Peters C, and Spits H. 2012 Transcriptional control of innate lymphoid cells. *Eur J Immunol* 42: 1916–1923. [PubMed: 22865043]
37. Grossman WJ, Verbsky JW, Barchet W, Colonna M, Atkinson JP, and Ley TJ. 2004 Human T regulatory cells can use the perforin pathway to cause autologous target cell death. *Immunity* 21: 589–601. [PubMed: 15485635]
38. Kumar V, and Sercarz E. 2001 An integrative model of regulation centered on recognition of TCR peptide/MHC complexes. *Immunol Rev* 182: 113–121. [PubMed: 11722628]
39. Madakamutil LT, Maricic I, Sercarz E, and Kumar V. 2003 Regulatory T cells control autoimmunity in vivo by inducing apoptotic depletion of activated pathogenic lymphocytes. *J Immunol* 170: 2985–2992. [PubMed: 12626551]
40. Gaur A, Ruberti G, Haspel R, Mayer JP, and Fathman CG. 1993 Requirement for CD8+ cells in T cell receptor peptide-induced clonal unresponsiveness. *Science* 259: 91–94. [PubMed: 8418501]
41. Tsai S, Shameli A, Yamanouchi J, Clemente-Casares X, Wang J, Serra P, Yang Y, Medarova Z, Moore A, and Santamaria P. 2010 Reversal of autoimmunity by boosting memory-like autoregulatory T cells. *Immunity* 32: 568–580. [PubMed: 20381385]
42. Pallett LJ, Davies J, Colbeck EJ, Robertson F, Hansi N, Easom NJW, Burton AR, Stegmann KA, Schurich A, Swadling L, Gill US, Male V, Luong T, Gander A, Davidson BR, Kennedy PTF, and Maini MK. 2017 IL-2(high) tissue-resident T cells in the human liver: Sentinels for hepatotropic infection. *J Exp Med* 214: 1567–1580. [PubMed: 28526759]
43. Liao W, Lin JX, and Leonard WJ. 2013 Interleukin-2 at the crossroads of effector responses, tolerance, and immunotherapy. *Immunity* 38: 13–25. [PubMed: 23352221]
44. Willerford DM, Chen J, Ferry JA, Davidson L, Ma A, and Alt FW. 1995 Interleukin-2 receptor alpha chain regulates the size and content of the peripheral lymphoid compartment. *Immunity* 3: 521–530. [PubMed: 7584142]
45. Sharfe N, Dadi HK, Shahar M, and Roifman CM. 1997 Human immune disorder arising from mutation of the alpha chain of the interleukin-2 receptor. *Proc Natl Acad Sci U S A* 94: 3168–3171. [PubMed: 9096364]
46. Malek TR, Yu A, Vincek V, Scibelli P, and Kong L. 2002 CD4 regulatory T cells prevent lethal autoimmunity in IL-2Rbeta-deficient mice. Implications for the nonredundant function of IL-2. *Immunity* 17: 167–178. [PubMed: 12196288]
47. Zhang Z, Gothe F, Pennamen P, James JR, McDonald D, Mata CP, Modis Y, Alazami AM, Acres M, Haller W, Bowen C, Doffinger R, Sinclair J, Brothers S, Zhang Y, Matthews HF, Naudion S, Pelluard F, Alajlan H, Yamazaki Y, Notarangelo LD, Thaventhiran JE, Engelhardt KR, Al-Mousa H, Hambleton S, Rooryck C, Smith KGC, and Lenardo MJ. 2019 Human interleukin-2 receptor beta mutations associated with defects in immunity and peripheral tolerance. *J Exp Med*.
48. Fernandez IZ, Baxter RM, Garcia-Perez JE, Vendrame E, Ranganath T, Kong DS, Lundquist K, Nguyen T, Ogolla S, Black J, Galambos C, Gumbart JC, Dawany N, Kelsen JR, de Zoeten EF, Quinones R, Eissa H, Verneris MR, Sullivan KE, Rochford R, Blish CA, Kedl RM, Dutmer CM, and Hsieh EWY. 2019 A novel human IL2RB mutation results in T and NK cell-driven immune dysregulation. *J Exp Med*.
49. Hinks A, Cobb J, Marion MC, Prahalad S, Sudman M, Bowes J, Martin P, Comeau ME, Sajuthi S, Andrews R, Brown M, Chen WM, Concannon P, Deloukas P, Edkins S, Eyre S, Gaffney PM, Guthery SL, Guthridge JM, Hunt SE, James JA, Keddache M, Moser KL, Nigrovic PA, Onengut-Gumuscu S, Onslow ML, Rose CD, Rich SS, Steel KJ, Wakeland EK, Wallace CA, Wedderburn LR, Woo P, J. I. A. R. Boston Children's, P. British Society of, G. Adolescent Rheumatology Study, S. Childhood Arthritis Prospective, S. Childhood Arthritis Response to Medication, R. German Society for Pediatric, J. I. A. G. E. Study, N. J. G. Registry, T. Study, C. United Kingdom Juvenile Idiopathic Arthritis Genetics, Bohnsack JF, Haas JP, Glass DN, Langefeld CD, Thomson W, and Thompson SD. 2013 Dense genotyping of immune-related disease regions identifies 14 new susceptibility loci for juvenile idiopathic arthritis. *Nat Genet* 45: 664–669. [PubMed: 23603761]
50. Moffatt MF, Gut IG, Demenais F, Strachan DP, Bouzigon E, Heath S, von Mutius E, Farrall M, Lathrop M, Cookson W, and G. Consortium. 2010 A large-scale, consortium-based genomewide association study of asthma. *N Engl J Med* 363: 1211–1221. [PubMed: 20860503]

51. Van Kaer L, Algood HMS, Singh K, Parekh VV, Greer MJ, Piazuelo MB, Weitkamp JH, Matta P, Chaturvedi R, Wilson KT, and Olivares-Villagomez D. 2014 CD8 α α (+) innate-type lymphocytes in the intestinal epithelium mediate mucosal immunity. *Immunity* 41: 451–464. [PubMed: 25220211]
52. Holz LE, Prier JE, Freestone D, Steiner TM, English K, Johnson DN, Mollard V, Cozijnsen A, Davey GM, Godfrey DI, Yui K, Mackay LK, Lahoud MH, Caminschi I, McFadden GI, Bertolino P, Fernandez-Ruiz D, and Heath WR. 2018 CD8(+) T Cell Activation Leads to Constitutive Formation of Liver Tissue-Resident Memory T Cells that Seed a Large and Flexible Niche in the Liver. *Cell Rep* 25: 68–79 e64. [PubMed: 30282039]
53. Thomas SY, Scanlon ST, Griewank KG, Constantinides MG, Savage AK, Barr KA, Meng F, Luster AD, and Bendelac A. 2011 PLZF induces an intravascular surveillance program mediated by long-lived LFA-1-ICAM-1 interactions. *J Exp Med* 208: 1179–1188. [PubMed: 21624939]
54. Golden-Mason L, Kelly AM, Doherty DG, Traynor O, McEntee G, Kelly J, Hegarty JE, and O'Farrelly C. 2004 Hepatic interleukin 15 (IL-15) expression: implications for local NK/NKT cell homeostasis and development. *Clin Exp Immunol* 138: 94–101. [PubMed: 15373910]
55. Holler PD, Yamagata T, Jiang W, Feuerer M, Benoist C, and Mathis D. 2007 The same genomic region conditions clonal deletion and clonal deviation to the CD8 α α and regulatory T cell lineages in NOD versus C57BL/6 mice. *Proc Natl Acad Sci U S A* 104: 7187–7192. [PubMed: 17438291]
56. Gangadharan D, Lambolez F, Attinger A, Wang-Zhu Y, Sullivan BA, and Cheroutre H. 2006 Identification of pre- and postselection TCR α beta+ intraepithelial lymphocyte precursors in the thymus. *Immunity* 25: 631–641. [PubMed: 17045820]
57. Judge AD, Zhang X, Fujii H, Surh CD, and Sprent J. 2002 Interleukin 15 controls both proliferation and survival of a subset of memory-phenotype CD8(+) T cells. *J Exp Med* 196: 935–946. [PubMed: 12370255]
58. Meraz MA, White JM, Sheehan KC, Bach EA, Rodig SJ, Dighe AS, Kaplan DH, Riley JK, Greenlund AC, Campbell D, Carver-Moore K, DuBois RN, Clark R, Aguet M, and Schreiber RD. 1996 Targeted disruption of the Stat1 gene in mice reveals unexpected physiologic specificity in the JAK-STAT signaling pathway. *Cell* 84: 431–442. [PubMed: 8608597]
59. Hofer MJ, Li W, Manders P, Terry R, Lim SL, King NJ, and Campbell IL. 2012 Mice deficient in STAT1 but not STAT2 or IRF9 develop a lethal CD4+ T-cell-mediated disease following infection with lymphocytic choriomeningitis virus. *J Virol* 86: 6932–6946. [PubMed: 22496215]
60. Arrenberg P, Halder R, Dai Y, Maricic I, and Kumar V. 2010 Oligoclonality and innate-like features in the TCR repertoire of type II NKT cells reactive to a beta-linked self-glycolipid. *Proc Natl Acad Sci U S A* 107: 10984–10989. [PubMed: 20534460]
61. Kuka M, Munitic I, and Ashwell JD. 2012 Identification and characterization of polyclonal α beta-T cells with dendritic cell properties. *Nat Commun* 3: 1223. [PubMed: 23187623]
62. Le Guen V, Judor JP, Boeffard F, Gauttier V, Ferry N, Soulillou JP, Brouard S, and Conchon S. 2017 Alloantigen gene transfer to hepatocytes promotes tolerance to pancreatic islet graft by inducing CD8(+) regulatory T cells. *J Hepatol* 66: 765–777. [PubMed: 27914923]
63. Takahashi T, Dejbakhsh-Jones S, and Strober S. 2006 Expression of CD161 (NKR-P1A) defines subsets of human CD4 and CD8 T cells with different functional activities. *J Immunol* 176: 211–216. [PubMed: 16365412]
64. Fergusson JR, Huhn MH, Swadling L, Walker LJ, Kurioka A, Llibre A, Bertoletti A, Hollander G, Newell EW, Davis MM, Sverremark-Ekstrom E, Powrie F, Capone S, Folgori A, Barnes E, Willberg CB, Ussher JE, and Klenerman P. 2016 CD161(int)CD8+ T cells: a novel population of highly functional, memory CD8+ T cells enriched within the gut. *Mucosal Immunol* 9: 401–413. [PubMed: 26220166]
65. Cunnusamy K, Baughman EJ, Franco J, Ortega SB, Sinha S, Chaudhary P, Greenberg BM, Frohman EM, and Karandikar NJ. 2014 Disease exacerbation of multiple sclerosis is characterized by loss of terminally differentiated autoregulatory CD8+ T cells. *Clin Immunol* 152: 115–126. [PubMed: 24657764]
66. Falanga YT, Frascoli M, Kaymaz Y, Forconi C, Ong'echa JM, Bailey JA, Berg LJ, and Moormann AM. 2017 High pathogen burden in childhood promotes the development of unconventional innate-like CD8+ T cells. *JCI Insight* 2.

67. Hansen SG, Piatak M Jr., Ventura AB, Hughes CM, Gilbride RM, Ford JC, Oswald K, Shoemaker R, Li Y, Lewis MS, Gilliam AN, Xu G, Whizin N, Burwitz BJ, Planer SL, Turner JM, Legasse AW, Axthelm MK, Nelson JA, Fruh K, Sacha JB, Estes JD, Keele BF, Edlefsen PT, Lifson JD, and Picker LJ. 2013 Immune clearance of highly pathogenic SIV infection. *Nature* 502: 100–104. [PubMed: 24025770]
68. St Leger AJ, Hansen AM, Karazum H, Horai R, Yu CR, Laurence A, Mayer-Barber KD, Silver P, Villasmil R, Egwuagu C, Datta SK, and Caspi RR. 2018 STAT-3-independent production of IL-17 by mouse innate-like alphabeta T cells controls ocular infection. *J Exp Med* 215: 1079–1090. [PubMed: 29490936]

KEY POINTS

- PLZF expression in CD8 $\alpha\alpha$ T_{unc} distinguishes them from conventional CD8 T cells
- CD8 $\alpha\alpha$ T_{unc} express NK cell markers, and dependent upon IL-2R β signaling
- CD8 $\alpha\alpha$ T_{unc} use perforin in a negative feedback mechanism to control autoimmunity

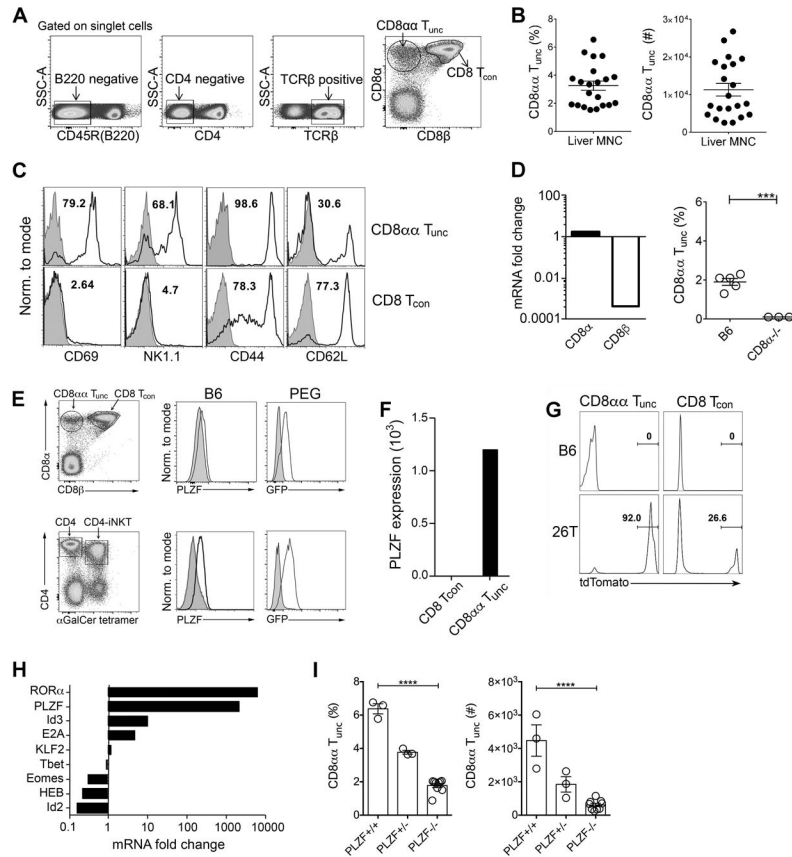


Figure 1. CD8 $\alpha\alpha$ T_{unc} are innate-like, memory T cells and are dependent upon PLZF. (A) Gating strategy for CD8 $\alpha\alpha$ T_{unc} in liver MNCs from naïve B6 mice. CD8 $\alpha\alpha$ T_{unc} were gated as singlet-B220⁻-CD4⁻-TCR β ⁺-CD8 α ⁺CD8 β ⁻ cells. (B) Cumulative percentage of hepatic CD8 $\alpha\alpha$ T_{unc} and numbers among TCR β ⁺ T cells in naïve B6 mice ($n = 21$). (C) Histograms overlay of individual marker expression in gated CD8 $\alpha\alpha$ T_{unc} and CD8 T_{con} (solid line) vs. isotype control (shaded). Numbers indicate percentage of positive cells in one of three mice. (D) (Left) Fold change of *CD8alpha* chain expression compared with *CD8beta* chain by qPCR in sorted hepatic CD8 $\alpha\alpha$ T_{unc} against CD8 T_{con}. (Right) Percentage of hepatic CD8 $\alpha\alpha$ T_{unc} in CD8 α ^{-/-} ($n = 3$) vs. B6 mice ($n = 5$). (E) Representative dot plots from one of three mice showing CD8 $\alpha\alpha$ T_{unc} and CD8 T_{con} (top) and CD4-iNKT cells (CD4⁺ α GalCer/CD1d tetramer⁺) and CD4 T cells (CD4⁺ α GalCer/CD1d tetramer⁻) (bottom). Histograms overlay of PLZF and GFP expression in gated hepatic CD8 $\alpha\alpha$ T_{unc} vs. CD8 T_{con} (top) and gated CD4-iNKT cells vs. CD4 T cells (bottom) from naïve B6 and PLZF-eGFP reporter (PEG) mice, respectively. CD8 $\alpha\alpha$ T_{unc} & CD4-iNKT cells, solid line; CD8 T_{con} & CD4 T cells, shaded histograms. (F) Relative expression of PLZF by qPCR in sorted hepatic CD8 $\alpha\alpha$ T_{unc} and CD8 T_{con} from naïve B6 mice ($n = 10$) using β actin reference gene. (G) Representative histograms of TdTomato expression in sorted hepatic CD8 $\alpha\alpha$ T_{unc} and CD8 T_{con} from B6 ($n = 5$) and *Pcre* \times R26T (26T) ($n = 5$) mice. Numbers indicate percentage of TdTomato⁺ cells. (H) Fold change of indicated immune genes expression by qPCR in sorted CD8 $\alpha\alpha$ T_{unc} against CD8 T_{con} from naïve B6 mice ($n = 10$). (I) Percentage and numbers of CD8 $\alpha\alpha$ T_{unc} from littermates (PLZF

+/+ and PLZF^{+/-}, $n = 3$) and homozygous PLZF^{-/-} mice ($n = 9$). Error is reported as SEM. Unpaired t tests were performed for data shown in D and I. ***P < 0.001; ****P < 0.0001. Data in each panel are representative of two or more independent experiments.

Author Manuscript

Author Manuscript

Author Manuscript

Author Manuscript

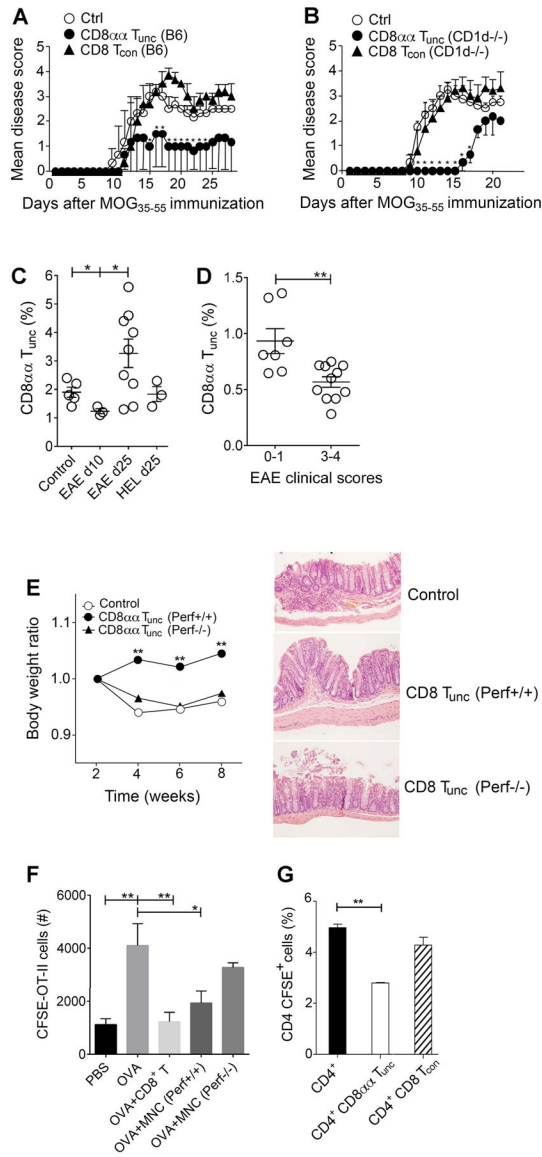


Figure 2. Adoptive transfer of CD8αα T_{unc} protects mice from EAE and colitis and they are expanded during EAE.

Sorted hepatic CD8αα T_{unc} or CD8 T_{con} ($1-2 \times 10^5$ /mouse) from naïve B6 (A) or naïve CD1d^{-/-} mice (B) were adoptively transferred into B6 recipients ($n = 3-5$) one day before EAE induction with MOG₃₅₋₅₅/CFA/PT and compared with the PBS-injected group. (C) CD8αα T_{unc} in MOG₃₅₋₅₅- or HEL₇₄₋₉₀-immunized B6 mice ($n = 3-9$) at day 10 or 25 or naïve B6 mice (Control, $n = 5$). (D) CD8αα T_{unc} at day 30 in B6 mice recovering from milder (scores 0-1) vs. severe (scores 3-4) EAE ($n = 18$ from two independent experiments). (E) Body weight ratio in Rag1^{-/-} mice after adoptive transfer of sorted CD4⁺CD25⁻CD45RB^{hi} T cells (4×10^5 /mouse) alone (Control) or co-injected with sorted hepatic CD8αα T_{unc} (2×10^5 /mouse) from either B6 (perf^{+/+}) or perforin^{-/-} (perf^{-/-}) mice ($n = 3$ /group). Representative H&E staining of colon sections ($\times 100$). (F) Numbers of CFSE-labeled OT-II CD4⁺ T cells recovered in spleen of B6 mice following their adoptive

transfer (1×10^6 /mouse) in control PBS ($n = 6$) or in OVA₃₂₃₋₃₃₉ peptide-injected ($n = 7$) or co-injected with positively selected CD8⁺ T cells (10×10^6 cells/mouse) ($n = 6$) or liver MNCs (8×10^6 cells/mouse) from B6 ($n = 5$) or perforin^{-/-} ($n = 3$) mice. **(G)** Percentage of CFSE-labeled CD4⁺ T cells recovered after 4 days of anti-CD3 stimulation of sorted CFSE-labeled CD4⁺ T cells (4×10^5 /well) cultured alone or together with either sorted hepatic CD8 $\alpha\alpha$ T_{unc} or CD8 T_{con} (1×10^5 /well) from naïve B6 mice. Error is reported as SEM. Student t test was performed for data shown in A and B, unpaired t test for data shown in C, D, E and G and ANOVA with Tukey's post-test for data shown in F. *P < 0.05; **P < 0.01. Data in each panel are representative of two or three independent experiments.

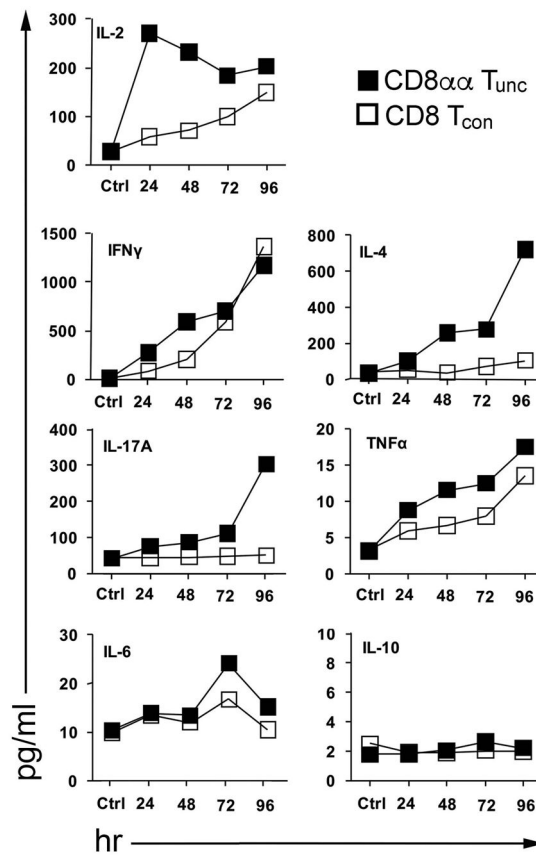


Figure 3. CD8 $\alpha\alpha$ T_{unc} secrete cytokines typical of innate-like cytotoxic CD8 T cells. Cytokines were quantified in supernatants at the indicated time points after *in vitro* stimulation with plate-bound anti-CD3 mAb (10 μ g/ml) of sorted hepatic CD8 $\alpha\alpha$ T_{unc} or CD8 T_{con} (1×10^5 cells/well) from naïve B6 mice. Data indicate concentrations (pg/ml) of cytokines detected by BD™ Cytometric Bead Array (CBA). These data are representative of two independent experiments.

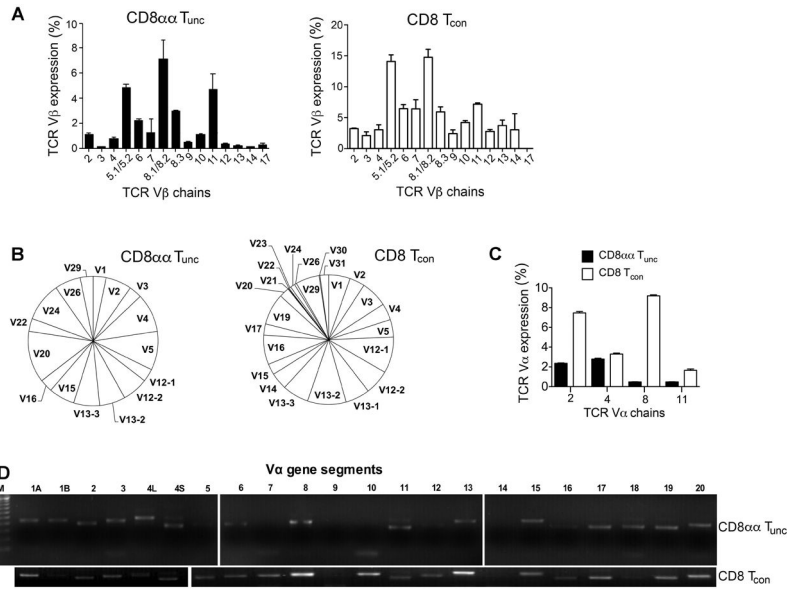


Figure 4. CD8αα T_{unc} are polyclonal and use diverse TCR α and β repertoires. (A) Percentage of sorted hepatic CD8αα T_{unc} (left) and CD8 T_{con} (right) isolated from naïve B6 mice ($n = 3$) expressing various TCR Vβ chains. (B) TRBV gene segment usage by sorted CD8αα T_{unc} (31 sequences, left) and CD8 T_{con} (7256 sequences, right) isolated from liver MNCs of naïve B6 mice ($n = 10$) as determined by high-throughput sequencing of the CDR3β regions. (C) Percentage of sorted hepatic CD8αα T_{unc} and CD8 T_{con} isolated from naïve B6 mice ($n = 3$) expressing various TCR Vα chains. (D) RT-PCR analysis of TCR Vα usage by sorted CD8αα T_{unc} and CD8 T_{con} isolated from liver MNCs of naïve B6 mice. Data in A, C and D are representative of two or three independent experiments.

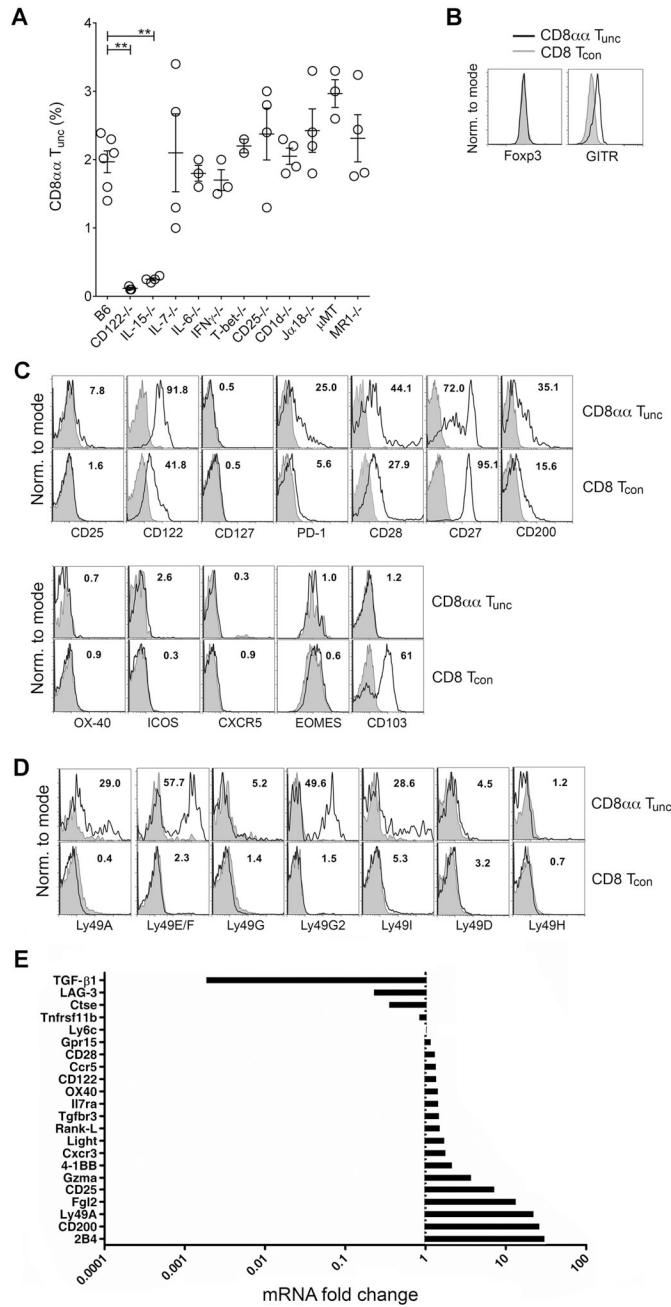


Figure 5. CD8 $\alpha\alpha$ T_{unc} are dependent on IL-15/IL-2R β signaling for their development/survival and express several immune regulatory markers. (A) Percentage of CD8 $\alpha\alpha$ T_{unc} in liver MNCs from indicated gene-deficient mice compared with naïve B6 mice ($n = 2-6$ mice per group) following gating strategy defined in Fig. 1A. ** $P < 0.01$, ANOVA with Bonferroni post-test. (B) Histograms overlay of Foxp3 and GITR expression in sorted CD8 $\alpha\alpha$ T_{unc} versus CD8 T_{con} in liver MNCs from one of three naïve B6 mice. (C) Histograms overlay of individual markers in gated CD8 $\alpha\alpha$ T_{unc} and CD8 T_{con} (solid line) vs. isotype control (shaded) in liver MNCs from one of three naïve B6 mice. Numbers indicate percentage of positive cells. (D) Histograms overlay for the expression of NK cell surface receptors in gated CD8 $\alpha\alpha$ T_{unc} and CD8 T_{con} (solid line) vs. isotype control

(shaded) in liver MNCs from one of three naïve B6 mice. Numbers indicate percentage of positive cells. (E) Fold change of indicated immune genes expression by qPCR in sorted CD8 $\alpha\alpha$ T_{unc} from liver MNCs of naïve B6 mice ($n = 10$) against CD8 T_{con}. Data in A-D are representative of two or three independent experiments.

Author Manuscript

Author Manuscript

Author Manuscript

Author Manuscript

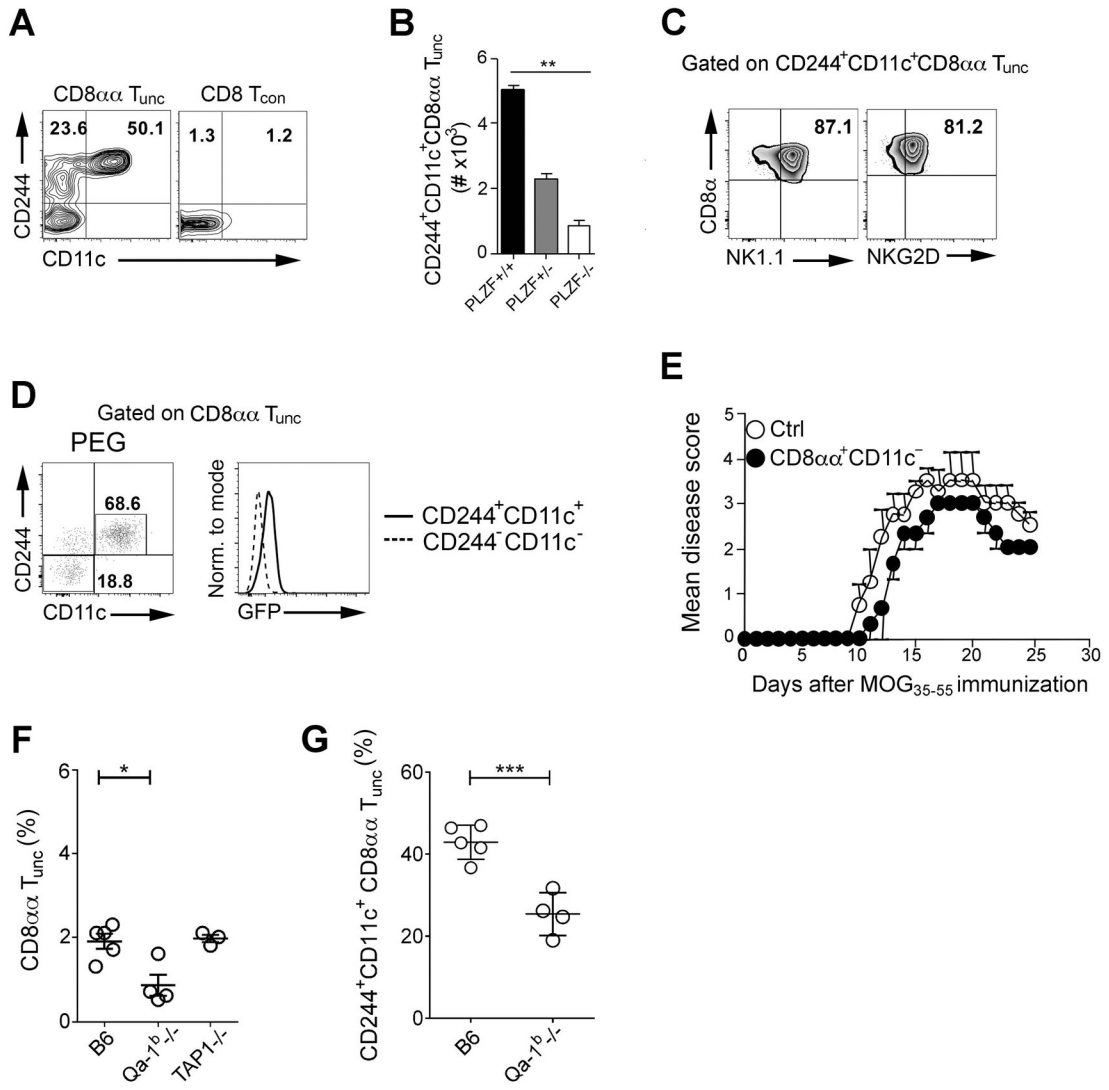


Figure 6. Co-expression of CD11c and CD244 is associated with a functionally distinct population within the heterogeneous population of CD8αα T_{unc}.
(A) Dot plots showing CD244 and CD11c expression by hepatic CD8αα T_{unc} and CD8 T_{con} from one of three naïve B6 mice gated as in Fig. 1A. Numbers indicate percentage of CD244⁺ or CD11c⁺CD244⁺. **(B)** Numbers of CD244⁺CD11c⁺ CD8αα T_{unc} in liver MNCs from littermates (PLZF^{+/+} and PLZF^{+/-}) and homozygous PLZF^{-/-} mice (*n* = 3-4 per group). **(C)** Dot plots showing NK1.1 and NKG2D expression on gated CD244⁺CD11c⁺ CD8αα T_{unc}. Numbers indicate percentage of positive cells in one of five mice. **(D)** *(Left)* Dot plot showing CD244 and CD11c expression by hepatic CD8αα T_{unc} from PEG mice gated as in Fig. 1A. Numbers indicate percentage of CD11c⁺CD244⁺ and CD11c⁻CD244⁻ cells in one of four mice. *(Right)* Histogram overlay of GFP expression by CD11c⁺CD244⁺ versus CD11c⁻CD244⁻ cells. **(E)** B6 mice (*n* = 3-5) were adoptive transfer with sorted hepatic CD8αα⁺ T_{unc} depleted of CD11c⁺ cells (CD8αα⁺CD11c⁻) from naïve B6 mice (2×10^5 /mouse) one day before EAE induction with MOG₃₅₋₅₅/CFA/PT. As positive control, EAE was induced in non-transferred B6 mice (*n* = 3-5). **(F)** Percentage of CD8αα T_{unc} in

liver MNCs from B6, Qa-1^{b-/-} and TAP1^{-/-} mice ($n= 3-5$ per group) gated as in Fig. 1A. (G) Percentage of gated CD244⁺CD11c⁺ CD8 $\alpha\alpha$ T_{unc} in liver MNCs from B6 ($n = 5$) and Qa-1^{b-/-} ($n = 4$) mice. Error is reported as SEM. Unpaired t tests were performed for data shown in B, F and G.*P < 0.05, **P < 0.01, ***P < 0.001. Data in each panel are representative of two or more independent experiments.

Author Manuscript

Author Manuscript

Author Manuscript

Author Manuscript

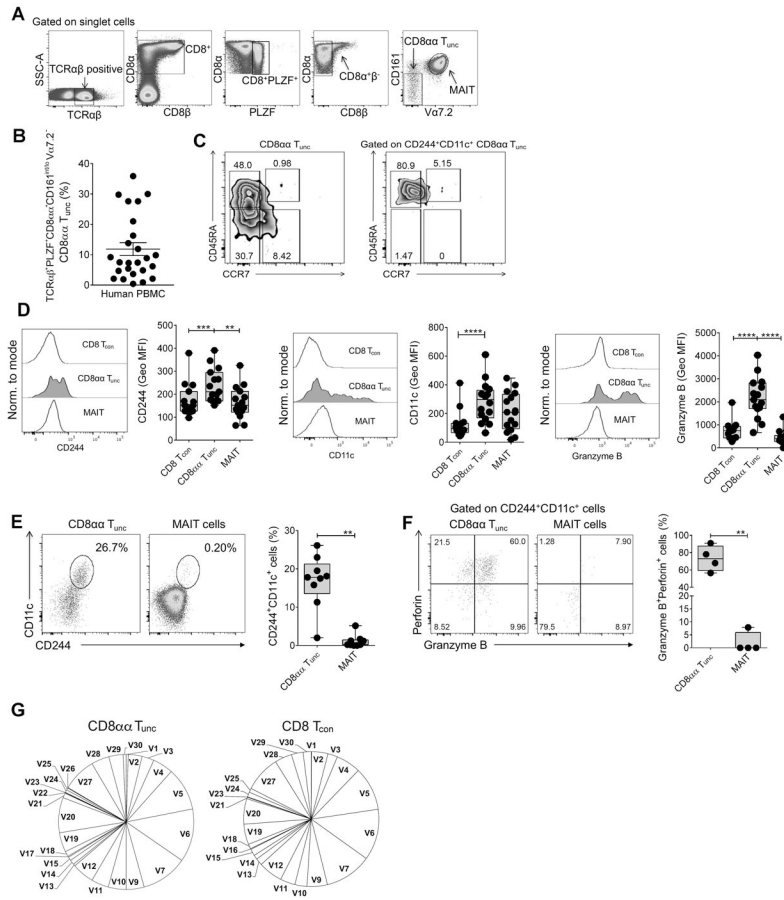


Figure 7. Presence of polyclonal CD8 $\alpha\alpha$ T_{unc} in PBMC from healthy subjects. (A) Gating strategy for human CD8 $\alpha\alpha$ T_{unc} in PBMC. CD8 $\alpha\alpha$ T_{unc} were gated based on exclusion of CD8 $\alpha\alpha$ ⁺ MAIT cells either Va7.2/Ja33⁺ or Va7.2/Ja33⁻ expressing higher levels of CD161 (CD161⁺⁺). Thus, CD8 $\alpha\alpha$ T_{unc} were defined as TCR $\alpha\beta$ ⁺PLZF⁺CD8 $\alpha\alpha$ ⁺CD161^{int/lo}. (B) Cumulative data of percentage of CD8 $\alpha\alpha$ T_{unc} in PBMC from healthy donors ($n = 25$) gated as in (A). (C) Representative dot plots of naïve (CD45RA⁺CCR7⁺), T_{CM} (CD45RA⁻CCR7⁺), T_{EM} (CD45RA⁻CCR7⁻) and T_{EMRA} (CD45RA⁺CCR7⁻) in gated CD8 $\alpha\alpha$ T_{unc} and CD244⁺CD11c⁺ CD8 $\alpha\alpha$ T_{unc}. Numbers indicate percentage of each subset from one of five healthy subjects. (D) Histograms and box plots (median, minimum and maximum values) of CD244, CD11c and Granzyme B expression in gated CD8 $\alpha\alpha$ T_{unc}, CD8 T_{con} and MAIT cells ($n = 13-16$) as in (A). (E) Co-expression of CD11c and CD244 on gated CD8 $\alpha\alpha$ T_{unc} and MAIT cells. Box plot showing percentages of CD244⁺CD11c⁺ cells on gated CD8 $\alpha\alpha$ T_{unc} and MAIT cells ($n = 9$). (F) Co-expression of Granzyme B and Perforin on gated CD244⁺CD11c⁺ CD8 $\alpha\alpha$ T_{unc} and CD244⁺CD11c⁺ MAIT cells. Box plot showing percentages of Granzyme B⁺Perforin⁺ in gated CD244⁺CD11c⁺ CD8 $\alpha\alpha$ T_{unc} and CD244⁺CD11c⁺ MAIT cells ($n = 4$). Each symbol in panels represents a single individual. (G) TRBV gene segment usage by sorted CD8 $\alpha\alpha$ T_{unc} (794 sequences, *left*) and CD8 T_{con} (12,244 sequences, *right*) isolated from PBMC of one healthy donor by high-throughput sequencing of the CDR3 β regions. Error is reported as SEM. ANOVA with Bonferroni post-

test was performed for data shown in D and paired t test for data shown in E and F. **P < 0.01; ***P < 0.001; ****P < 0.0001.

Author Manuscript

Author Manuscript

Author Manuscript

Author Manuscript